Flow-Through Cell for Ion-selective Electrodes

Åbo Akademi University

Faculty of Science and Engineering

Enahoro Aigboje Asein

Master's programme in Excellence in Analytical Chemistry

Degree project in Analytical chemistry, 30 credits

Supervisor: **Zekra Mousavi** (Åbo Akademi University)

Co-supervisors: **Johan Bobacka** (Åbo Akademi University)

Agnes Heering (University of Tartu)

June 2023

Table of Contents

Preface

The work in this thesis was performed at the Laboratory of Molecular Science and Engineering at Åbo Akademi University during the 2022/23 academic year. The thesis is the final part of the Erasmus Mundus Joint Master's Degree program Excellence in Analytical Chemistry (EACH), an EU-funded program in collaboration with University of Tartu (EST), Åbo Akademi University (FIN), University Claude Bernard Lyon 1 (FRA), and Uppsala University (SWE).

I would like to extend my most sincere gratitude to my supervisor, Docent Zekra Mousavi, for her time, patience, and support throughout this work. You taught me a lot during our time working together and I have learned a lot that will undoubtedly help me become a good scientist. I would also like to thank my co-supervisors, Prof. Johan Bobacka and Dr. Agnes Heering, for their continuous feedback and support. You have all contributed significantly to the results and writing of this master's thesis. Thank you.

The last two years have been a wonderful and unforgettable experience in so many areas. Thank you to my classmates, friends, and everyone involved in the EACH program for contributing to that experience and helping me go through it successfully. To my family and friends, who have remained supportive despite being far away, thank you.

List of Abbreviations and Symbols

a_{Cl^-}	Chloride ion activity
E_{Ag/Ag^+}	Electric potential of the Ag/AgCl electrode
φ	Phase angle
A, B	Constants in the limiting law of the Debye-Hückel theory
A^-	Anionic dopant
Ag/AgCl	Silver/Silver chloride
a_i	Activity of primary ion (*i*)
a_j	Activity of interfering ion (*j*)
$a_{Kjel,i}$	Kjelland parameter of ion *i*
BGE	Background electrolyte
C^+	Cationic analyte
CC	Carbon cloth
CC-ISEs	Carbon cloth-based ion-selective electrodes
C_{dl}	Double layer capacitance
C_i	Concentration of ion *i*
Cl-ISE	Chloride ion-selective electrode
Cl-ISM	Chloride ion-selective membrane
CNTs	Carbon nanotubes
CP	Conducting polymer
CWE	Coated-wire electrode
DE	Disk electrode
DMPP	2,2-dimethoxy-2-phenylacetophenone
DOS	Dioctyl sebacate (bis(2-ethylhexyl) sebacate)
E_0	Amplitude of the applied potential
E^0	Standard potential
E_{cell}	Net cell potential
EIS	Electrochemical impedance spectroscopy
$E_{membrane}$	Membrane potential
E_t	Time-dependent potential
F	Faraday constant (96 485.33 $C \cdot mol^{-1}$)
FIM	Fixed interference method
GC	Glassy carbon

I_0	Amplitude of the current response
ISE	Ion-selective electrode
ISM	Ion-selective membrane
I_t	Time-dependent current
J	Ionic strength of the sample
j	Imaginary number
K-ISE	Potassium ion-selective electrode
K-ISM	Potassium ion-selective membrane
$K_{i,j}$	Selectivity coefficient
KTFPB	Potassium tetrakis[3,5-bis(trifluoromethyl)phenyl] borate
L	Ionophore
LJP	Liquid junction potential
MWCNT	Multiwalled carbon nanotube
nC^+	Cationic non-analyte
nC^-	Anionic non-analyte
oNPOE	2-nitrophenyl octyl ether
PC	Polycarbonate
PEDOT	Poly (3,4-ethylenedioxythiophene)
PET	Polyethylene terephthalate
POT	Poly(3-octylthiophene)
PSS	Polystyrene sulfonate
PTFE	Polytetrafluoroethylene
PVAc	Polyvinyl acetate
PVB	Polyvinyl butyral
PVC	Polyvinyl chloride
R	Universal gas constant (8.314 $J \cdot mol^{-1} \cdot K^{-1}$)
R^-	Lipophilic anion
R^2	Coefficient of determination
R_{ct}	Charge transfer resistance
R_s	Solution resistance
SCISE	Solid-contact ion-selective electrode
SHE	Standard hydrogen electrode
SSM	Separate solution method

T	Absolute temperature
TDMAC	Tridodecylmethylammonium chloride
THF	Tetrahydrofuran
VAc	Vinyl acetate monomer
Z	Impedance
Z'	Real component of the impedance
Z''	Imaginary component of the impedance
Z_0	Magnitude of the impedance
z_i	Charge of primary ion (i)
z_j	Charge of interfering ion (j)
Z_W	Warburg impedance
γ_i	Activity coefficient of ion i
ω	Radial (or angular) frequency

Abstract

This research work describes a novel flow-through all-solid-state potentiometric device that consists of solid-contact ion-selective electrodes and a solid-state planar reference electrode. The device is capable of measuring ionic concentrations in small sample volumes. Planar potassium ion-selective electrodes (K-ISEs) and chloride ion-selective electrodes (Cl-ISEs) were made using carbon cloth (CC) as ion-to-electron signal transducer (CC-ISEs). Polyvinyl butyral/sodium chloride (PVB/NaCl)-based and polyvinyl acetate/potassium chloride (PVAc/KCl) composite-based reference electrodes were prepared using silver/silver chloride disk electrodes and characterized. The PVAc/KCl composite-based reference electrode showed superior performance and was selected for use in the flow-through device. Carbon cloth and polycarbonate (PC) were tested as substrates for the fabrication of the planar PVAc/KCl composite-based reference electrode. The reference electrode made using the CC substrate (CC-RE) performed well when used with either an external commercial reference electrode or a chloride ion-selective electrode. However, the construction and assembly of the CC-RE made it perform poorly when combined with a CC-ISE in one cell. The PC-based reference electrode (PC-RE) solved the issues associated with the CC-RE and performed well when combined with CC-ISEs in the complete flow-through potentiometric device. When measured against the PC-RE, the potassium and chloride CC-ISEs (K- and Cl-ISEs) consistently showed fast and stable near-Nernstian responses, good R^2 values, and high within-day repeatability in the 10^{-3} M to 10^{-1} M KCl concentration range. The use of valinomycin as ionophore in the studied K-ISEs resulted in excellent selectivity for the electrodes in the presence of interfering ions such as Na^+, Mg^+, and Ca^{2+}. Whereas the Cl-ISEs based on the ion exchanger tridodecylmethylammonium chloride (TDMAC) showed relatively poor selectivity in the presence of interfering ions such as bicarbonate (HCO^{3-}) and lactate ($C_3H5O_3^-$). These ions were selected for the selectivity measurements due to their significant presence in sweat samples that are meant to be measured using the flow-through device. The standard potentials of both potassium and chloride CC-ISEs demonstrated poor reproducibility in between-electrode and between-day measurements. Results from the electrochemical impedance spectroscopy measurements, carried out using the K-ISEs, showed that the resistance of the valinomycin-based potassium ion-selective membrane (ISM) is relatively high in these electrodes compared to the values reported in the literature. In addition, electrodes made in a similar way and are supposed to be identical exhibited different values of ISM resistance. This can be attributed to errors in the manual fabrication of the electrodes. Despite

the high (charge transfer) resistance values of the ISMs, the CC-ISEs showed fast and relatively stable potentiometric responses.

Keywords: Flow-through cell; Potentiometric sensing; Planar solid-contact ion-selective electrodes; Planar solid-state reference electrodes

1 Introduction

Wearable sensors/devices, also referred to as wearables, have experienced widespread adoption, evidenced by over 400 million units shipped annually in the last three years[1]. Biological samples such as sweat and interstitial fluid contain analytes such as potassium and chloride ions; real-time continuous measurement of their concentrations could provide relevant information for health monitoring[2, 3].

Loss of potassium through sweating could result in hypokalaemia, increasing the risk for hypertension[4] and sweat chloride testing is a standard method for diagnosing cystic fibrosis[5]. Typical concentrations of potassium and chloride ions in sweat (2 mM to 8 mM and 10 mM to 90 mM[6], respectively) are high enough for reliable detection by the conventional potentiometry technique[7]. One advantage of potentiometry as an analytical technique is its simplicity. Requiring only a potentiometer to measure the potential difference between the ion-selective electrode (ISE) and reference electrode makes its implementation in wearables more feasible. However, challenges in developing miniaturised solid-state potentiometric devices still need to be overcome.

One issue with most well-performing sweat sensing devices in the literature[8, 9] is the use of a silver/silver chloride (Ag/AgCl) reference electrode with low chloride salt concentrations. This results in unstable responses and shorter electrode lifetime. Another issue is the typical planar construction of most developed sweat-sensing devices. This construction typically requires additional sweat sampling devices to address the challenge of mixing old and fresh samples during continuous measurement[10, 11].

This thesis aims to demonstrate a proof-of-concept for a planar flow-through device operating with a solid-state Ag/AgCl reference electrode, with a higher chloride salt concentration needed for stable potential, together with two ISEs. The flow-through design inherently solves the sampling challenge without requiring an additional sampling device. Additionally, using a flow-through design could allow for isolating the sensing components, preventing direct skin contact, while measuring smaller sample volumes than in the typical planar designs.

In a previous work, potassium ion-selective electrode (K-ISE) in a flow-through cell was used with an external commercial reference electrode[12, 13]. The work in this thesis builds upon that work by integrating a planar solid-state reference electrode in the sensing platform. In addition

to the previously used K-ISE, a chloride ion-selective electrode (Cl-ISE) was also introduced in this study for a true flow-through operation. The developed solid-state device can reliably and continuously measure ion concentrations in small fluid volumes. The use of flexible carbon cloth as the ion-to-electron transducer in both K- and Cl-ISEs, promotes the design's usability in wearables. Based on the work done during this thesis, printing technologies could later be used for more reproducible and larger-scale production of smaller ion sensing devices.

The first stage of the experimental work carried out in this thesis involved testing different solid-state reference electrodes for possible use in the flow-through device. The second stage focused on designing a planar solid-state reference electrode based on a polymer/inorganic salt composite[14, 15] and combining it with potassium and chloride ISEs. In the final stage, the performance of the whole flow-through device was studied and evaluated.

The following pages provide a written statement of the experimental work as well as the theoretical framework it is based on. **Section 2** provides a general overview of chemical sensors and potentiometric sensing. **Section 3** provides more specific details on the experimental setup and flow-through cell designs used throughout this thesis work. **Sections 4 and 5** give an evaluation of the obtained results.

2 Theoretical Background

Ears, eyes, nose, skin, and tongue, the five primary sensors in the human body, can detect certain stimuli (changes and properties) in our immediate environment. Although the evolution of our sensory system has let us survive and thrive in our environment, changes in our world are significantly outpacing our evolutionary capacity. That is why developing sensors with capabilities extending beyond us is required. The developed sensors fall into two broad categories: physical and chemical, which respond to physical and chemical changes, respectively. Physical sensors such as mass balances and thermometers are the most familiar ones in everyday life. Though, the discussion of chemical sensors is most relevant to this thesis.

2.1 Chemical Sensors

Chemical sensors are developed to convert the chemical information from their environment into a readable output signal[16]. As schematically shown in Figure 1, chemical interactions at a **receptor in the chemical sensor** are converted into a physical quantity through a **transduction** step. The response of the physical quantity to changes in the chemical environment may be high enough to be measured reliably, but sometimes, it is so low that an **amplification** step is used to record a reliable signal. The final step is **information processing**, which should give some description of the sensor's chemical environment[17, 18].

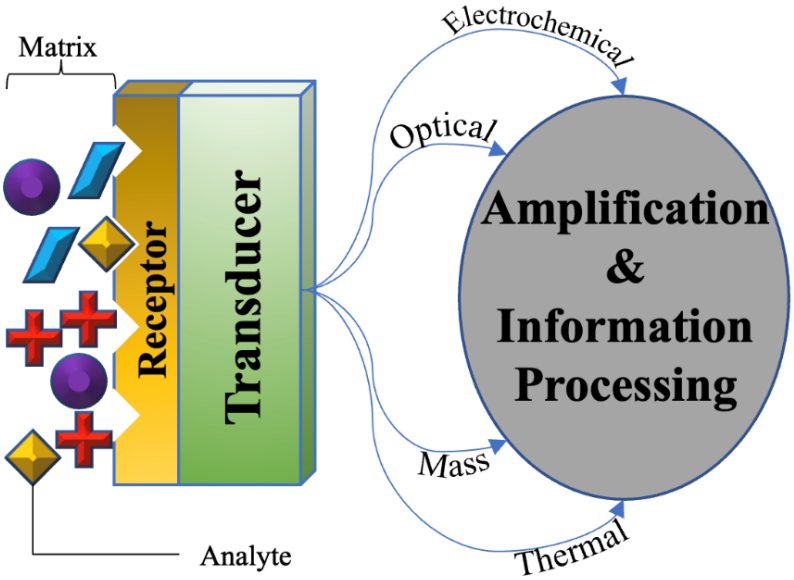

Figure 1. Schematic illustration of the elements in a chemical sensor and the processes involved in the system.

Receptors can be grouped according to the analyte type they recognise[18] or their selectivity method[17] (Table 1).

Table 1. Classification of receptors used in chemical sensors.

Analyte Types	Selectivity Methods
- Ionic	- Equilibrium-based
- Molecular	- Kinetic-based
- Biological	- Mass transport

Although receptors are important for analyte recognition, chemical sensors are primarily classified based on their transducer element. The main groups are[16]:

i) Electrochemical sensors: The chemical nature of the sample induces a change in electrical properties such as potential, current, and conductivity.
ii) Optical sensors: Optical properties such as reflectance, absorbance, and transmittance are related to the sample's chemical composition.
iii) Mass sensors: A change in mass at the receptor is used to identify and quantify analyte binding.
iv) Thermal sensors: The amount of heat generated or absorbed is related to the chemical entities present.

This thesis's focus, potentiometric ion sensors or ion-selective electrodes (ISEs), falls under the electrochemical sensors group with receptors that respond to ionic analytes. The signal in a potentiometric ion sensor setup is the potential between the ISE and a reference electrode measured under the condition of zero current.[17].

2.2 Ion-Selective Electrodes

An ion-selective electrode (ISE) is an indicator electrode that preferentially responds to a specific ion in the sample and converts the concentration (activity) of the ion into a measurable electrical potential signal. Although potentiometry can be applied to detect neutral species[17], the fundamental principle of operation relies on ionic detection.[18]. For targeted ion detection, especially in the presence of other ions, an ion-selective membrane (ISM) is used to ensure that the potential depends only on the activity of the target ion in the sample. The membrane potential will depend on the phase boundary potential at the ISM ⎪ sample solution interface[19].

The most common sensor based on potentiometry is the pH glass electrode which was invented in 1906, making it the first device in the history of ISEs[17]. Since then, other ISEs have been developed for a wide range of analytes and applications. Examples of such applications and analytes are blood serum analysis (pH, K^+, Cl^-), environmental monitoring (pH, Pb^{2+}, NO_3^-), and power station operations (pH, Na^+)[20].

Primary ISEs, designed to detect their target analyte ions in the sample, can be classified into three main types based on their ISM – glass, solid-state membrane, and liquid membrane electrodes[21, 22]. Liquid membrane-based electrodes are the most versatile type that can detect a wide range of analytes by varying the membrane components.

Composition of Liquid Membranes

The most important part of an ISE is the ISM. The membrane components should be highly hydrophobic (assuming measurements are done in aqueous samples) to prevent leaching of the membrane components. On the other hand, the membrane should be selectively permeable to allow the inflow of the analyte ion. The so-called solvent polymeric membrane is one kind of ion-selective membranes, which usually consists of a poly(vinyl) chloride (PVC) (Figure 2a) matrix containing a neutral ionophore or an ion exchanger that makes the membrane selective to a certain ion.

Ionophores are macrocyclic molecules or crown ethers which bind reversibly to their analytes. A proper ionophore reversibly binds the analyte ion and forms a strong complex, resulting in a potential across the membrane. Ionophores have been developed and used in membranes for ion-selective sensing of a wide range of analytes[17]. One ionophore that has shown very impressive performance in previous research is valinomycin (Figure 2b), utilized for potassium ion sensing[23]. When a neutral ionophore (such as valinomycin) is used in the membrane, a lipophilic salt such as potassium tetrakis[3,5-bis(trifluoromethyl)phenyl] borate (KTFPB) (Figure 2c) is added to ensure the permselectivity of the ISM. This means preventing interference from counter ions (Donnan exclusion) in order to have an efficient electrode performance. The selectivity improvement comes from decreased membrane resistance and decreased interference from non-analyte ions. The lipophilic salt-to-ionophore ratio is chosen to be high enough to improve selectivity while being low enough to prevent significant ion exchange behaviour by the salt[24]. Other components are also added to improve the physical and mechanical properties of the membrane. One of these components is the plasticiser, such as bis(2-ethylhexyl) sebacate, also known as dioctyl sebacate (DOS) (Figure 2d) and

2-nitrophenyl octyl ether (oNPOE) (Figure 2e) which are used to make the membrane more flexible and durable[25].

In the case of ion exchangers, the analyte ions in the sample replace mobile ions with the same charge in the membrane. The ideally selective ionic exchange results in a potential across the membrane proportional to the analyte's activity[17]. Tridodecylmethylammonium chloride (TDMAC) (Figure 2f) is a chloride anion exchanger used to prepare chloride ISEs.

All the membrane components are dissolved in an organic solvent with a low boiling point, such as tetrahydrofuran (THF) (Figure 2g).

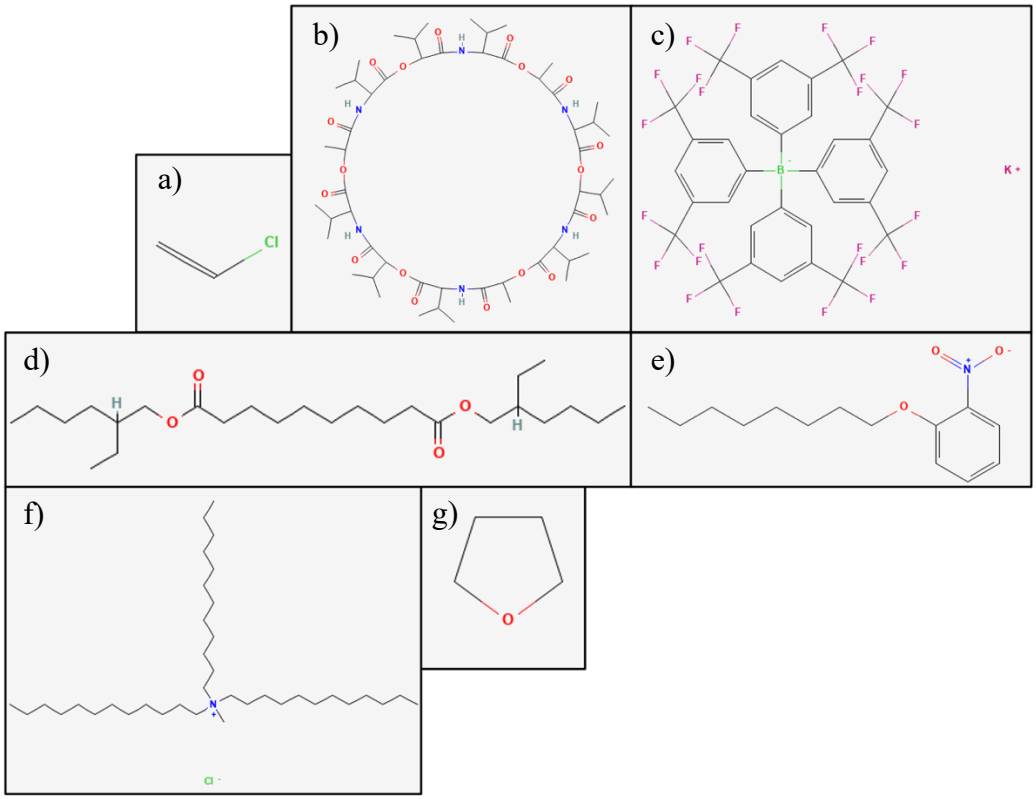

Figure 2. 2D chemical structures of some PVC-based ISM components. a) Poly(vinyl) chloride[26] b) Valinomycin[27] c) Potassium tetrakis[3,5-bis(trifluoromethyl)phenyl]borate[28] d) Bis(2-ethylhexyl) sebacate[29] e) 2-Nitrophenyl octyl ether[30] f) Tridodecylmethylammonium chloride[31] g) Tetrahydrofuran[32].

2.2.1 Signal Transduction in Ion-Selective Electrodes

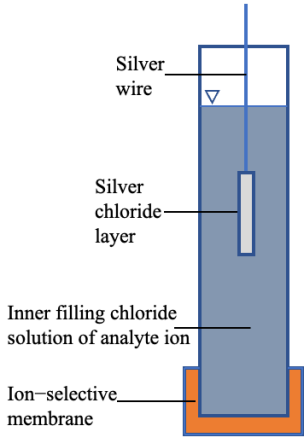

Figure 3. Schematic illustration of a conventional ion-selective electrode.

In ion-selective electrodes, the signal transduction element is necessary to convert ionic responses to electronic signals. In a conventional ISE (Figure 3), an ion-selective membrane is attached to the end of a tube filled with an inner filling solution that functions as a charge carrier between the ISM and the inner reference electrode.

The ion-to-electron transduction mechanism in a conventional ISE is based on electrodes of the second kind where a metal electrode is coated with an insoluble/sparingly soluble salt of the metal. The Ag/AgCl electrode is the most common electrode based on this mechanism. With all other variables constant, the electric potential of this electrode (E_{Ag/Ag^+}) depends only on the chloride ion activity (a_{Cl^-}) of the inner filling solution in contact with the electrode (Eq 2.1)[17]. Hence, if the chloride ion activity of the inner filling solution is kept constant, the electric potential of the electrode is constant.

$$E_{Ag/Ag^+} = Constant - \frac{R \cdot T}{F} \cdot ln\, a_{Cl^-} \qquad (Eq\ 2.1)$$

R is the universal gas constant (8.314 J·mol^{-1}·K^{-1}), T is the absolute temperature, and F is the Faraday constant (96 485.33 C·mol^{-1}).

The inner filling solution also contains a constant activity of the analyte ion resulting in a constant potential across the inner filling solution | ISM interface. The chloride ion equilibrium at the Ag/AgCl | inner filling solution interface and the overall Ag/AgCl electrode reaction (Eq 2.2) are responsible for the ion-to-electron transduction (Figure 4a).

$$AgCl_{(s)} + e^- \rightleftharpoons Ag_{(s)} + Cl^- \qquad (Eq\ 2.2)$$

However, the presence of inner filling solution in the structure of conventional ISEs gives rise to some significant drawbacks such as inability to use the electrode in different positions because the solution must remain in contact with the ISM, evaporation of the filling solution, and difficulty to miniaturise. For these reasons, advances in sensors research have tried to replace the inner filling solutions with solid-contact transducers. This is a significant step towards miniaturised and more robust electrochemical sensors[33, 34]. Introducing the coated-wire electrode (CWE), and later the solid-contact ISE (SCISE) concept opened a new route towards the construction of robust, maintenance-free, and reliable all-solid-state ISEs. In the

case of a CWE[35, 36], the ISM is directly attached to the surface of an electronic conductor such as platinum, copper, or glassy carbon. The CWEs operate according to a double-layer capacitance mechanism (Figure 4b). Irreproducibility and drift of the potential are among the drawbacks of the CWE that were attributed to the high charge-transfer resistance at the conducting substrate | ISM interface[17]. To solve these problems, a solid layer between the ISM and the electronic conductor was used in the SCISEs for ion-to-electron transduction. Different materials such as porous and nanostructured carbon materials, e.g., macroporous carbon[37], carbon nanotubes (CNTs)[38], graphene[39], fullerenes[40], and carbon cloth[41] have been used for this purpose. When using these materials as solid contact, the ion-to-electron signal transduction mechanism is also ascribed to the formation of an electrical double layer between the ISM and the solid contact layer (Figure 4b). However, the high surface area provided by the carbon materials results in an amplified double layer capacitance. Furthermore, other materials such as conducting polymers (CPs) and functionalised CPs were used as ion-to-electron transducers for preparing SCISEs[42, 43]. In this case, the ion-to-electron transduction process is based on the electronic conductivity and high redox capacitance of these materials (Figure 4c and Figure 4d).

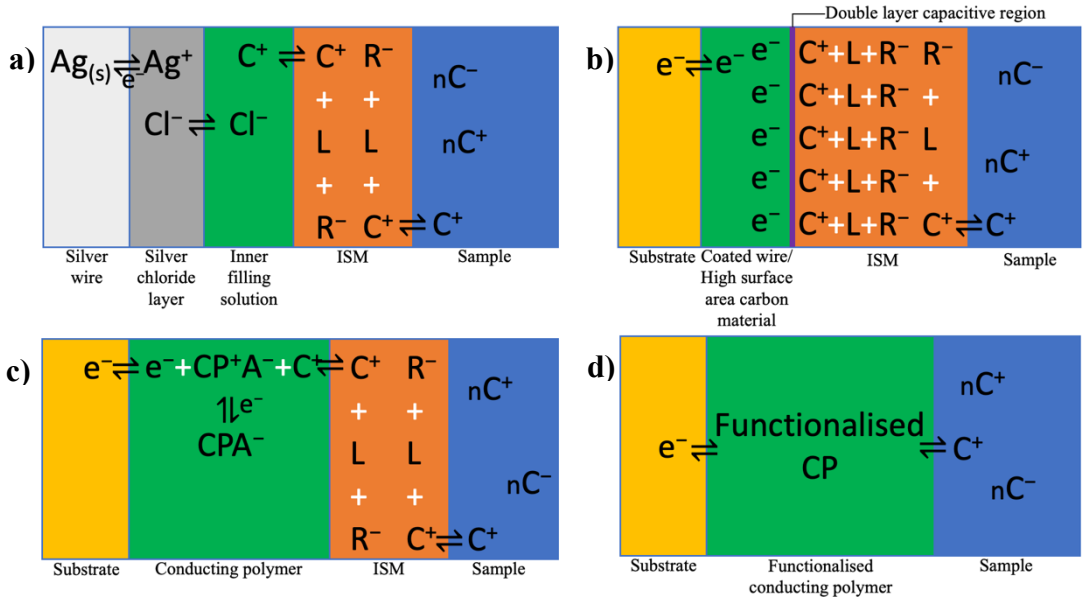

Figure 4. Ion-to-electron transduction mechanism in a) ISE with inner filling solution; b) coated wire electrode and ISE with high surface area carbon materials as solid contact; c) conducting polymer-based ISE; d) functionalised conducting polymer-based ISE. L: ionophore; R^-: Lipophilic anion; C^+: cationic analyte; nC^+: cationic non-analyte (matrix component); nC^-: anionic non-analyte (matrix component); CP: conducting polymer; A^-: anionic dopant; e^-: electron.

2.3 Reference Electrodes

2.3.1 Conventional Reference Electrodes

In an electrochemical measurement, the reference electrode is a crucial component that establishes precise, stable, and reproducible potentials independent of the composition of the sample[44].

The fundamental reference electrode is the standard hydrogen electrode (SHE), an ideal electrode consisting of hydrogen gas at 1 atm bubbled through a solution in which the hydrogen ion activity is 1. This electrode has a defined standard potential of 0 V at all temperatures. The standard reduction potential of other electrodes and redox couples are defined against the SHE. However, the SHE is impractical for real-life scenarios; hence other reference electrodes are used.

The two most common practical conventional reference electrodes, the mercury/mercurous chloride (calomel) electrode and the silver/silver chloride (Ag/AgCl) electrode both operate as electrodes of the second kind (Eq 2.2). Due to the toxic nature of mercury, the Ag/AgCl reference electrode is more favoured.

Silver/Silver Chloride Reference Electrode

The Ag/AgCl reference electrode consists of silver chloride on a silver wire in contact with a solution of chloride ions, typically potassium chloride (KCl) (Figure 5). The activity of chloride ion in the solution determines the potential of the electrode (Eq 2.1). A porous frit serves as a salt bridge between the inner filling solution and the sample solution in which the reference electrode is immersed in. The potassium chloride solution is used as inner filling solution because of the similar mobilities of potassium and chloride ions[45]. The similar mobilities helps to minimise the liquid-junction potential (LJP) (2.4).

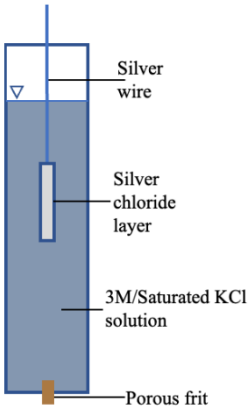

Figure 5. Schematic illustration of a conventional silver/silver chloride reference electrode.

2.3.2 Solid-State Reference Electrodes

A conventional reference electrode such as the Ag/AgCl/3M KCl, with the inner filling solution as a basic component, has several drawbacks which makes it expensive to manufacture and difficult to maintain and miniaturise[45]. To move away from the conventional reference electrode, some suggestions based on the Ag/AgCl electrode have been proposed. The

Ag/AgCl electrode has been the foundation for these proposals due to its high exchange current density, low polarizability, simplicity, and cheapness[46]. Some key challenges an ideal solid-state reference electrode should address, especially for miniaturisation are:

- Sufficient silver and silver chloride for the expected electrode lifetime.
- Sufficient chloride concentration in the solid layer in contact with the Ag/AgCl layer.
- Large enough surface area of the electrode in contact with the sample for higher stability of the potentiometric response.
- Slow but adequate ion flux from the solid layer into the sample to avoid significant depletion of chloride ions in the solid layer and contamination of the sample.

Examples of effective strategies to achieve a reliable solid-state reference electrode include:

- Ag/AgCl electrode in a vinyl ester resin doped with KCl[47]
- Lipophilic salts in a PVC membrane drop cast onto an Ag/AgCl electrode[48]
- PVC membrane containing ionic liquids on planar Ag/AgCl electrodes[49]
- Polyvinyl butyral (PVB) membrane containing sodium chloride (NaCl) on planar Ag/AgCl electrodes[8, 9]
- Ag/AgCl within a polymer matrix containing KCl[14, 15]

PVB-Based Planar Reference Electrode

One method for maintaining stable chloride concentration in miniaturised reference electrodes uses NaCl within a PVB membrane[8, 9]. Methanol, a quick-evaporating solvent, was used for making the membrane cocktail. However, the solubility of NaCl in methanol is relatively low (1.40 g/100) vs. 36.0 g/100 g in water, at 25 °C[50]; therefore, the concentration of chloride within the membrane is also low. The low solubility and unequal mobilities of sodium and chloride ions results in unstable long-term potentials and potential drift during measurement. For this reason, research was done to minimise the drift by adding an adsorption barrier such as CNTs which reduce the ion flux[51, 52].

Solid-state Composite Reference Electrode

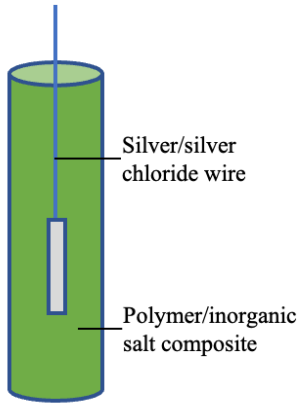

Figure 6. Schematic illustration of a solid-state composite reference electrode.

In this type of solid-state reference electrode, the KCl filling solution in the conventional Ag/AgCl reference electrode is replaced by a polymer/inorganic salt composite (Figure 6). An Ag/AgCl wire is inserted in the polymer matrix as the reference element. The polymer (such as polyvinyl acetate)/inorganic salt (KCl) composite maintains the chloride concentration needed for stable and reproducible potentials and acts also as a contact with the sample solution. The sufficient chloride concentration offered by this design resulted in a good analytical performance in terms of potential stability, even with varying sample composition. The ability to use the electrode in any position, minimal need for maintenance, low salt leakage from the composite, and ease of manufacturing make the electrode design very robust and reliable. The electrode can be prepared by chemical polymerisation[14] or injection moulding[15].

2.4 Working Principle of Potentiometry

Potentiometry is an electroanalytical technique whose simplicity has made it one of the most widely used analytical techniques[53]. The technique measures the potential difference between one or more indicator electrodes and a reference electrode at equilibrium (Figure 7). At equilibrium, the net current flowing between the electrodes is negligible (virtually zero), and hence, no redox reactions contribute to the measured potential difference. The equilibrium condition is achieved using a high input impedance potentiometer, which draws very little current, to measure the potential difference[22]. The magnitude of the measured potential in a typical electrochemical cell depends on three parameters:

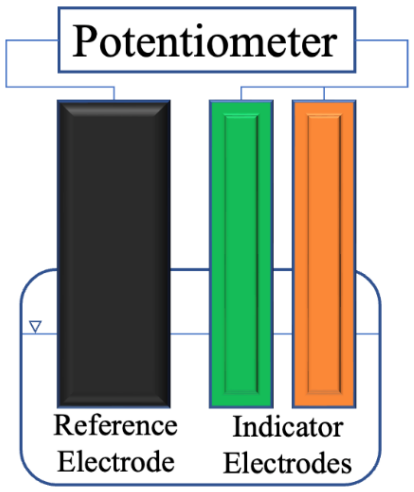

Figure 7. Simplified illustration of a potentiometric measurement setup.

- *Indicator electrode potential*: The indicator electrode in contact with the sample solution has a potential, E_{ind}, which depends on the analyte activity.

- *Reference electrode potential*: The reference electrode has a potential, E_{ref}, which is (ideally) constant and independent of the sample composition and analyte activity.
- *Liquid-junction potential (LJP)*: It develops at a liquid junction, an interface between two dissimilar solutions. The liquid junction creates electrical contact by allowing the slow exchange of ions between the reference and sample solutions[54]. Different ionic mobilities across the junction results in a potential, E_j, which can be modelled with the Henderson equation[54]. In practice, conventional potentiometry uses high concentration inner filling solutions with ions of similar mobilities (e.g., potassium chloride and lithium acetate in conventional Ag/AgCl reference electrodes) to minimise the LJP which allows it to be considered as negligible[45, 55]. However, estimation might be necessary in certain conditions such as measurements at low/trace concentrations.

The potentials described above are related to the net potential of the electrochemical cell, E_{cell}, measured by the potentiometer, using the equation below[22]:

$$E_{\text{cell}} = E_{\text{ind}} - E_{\text{ref}} + E_{\text{j}} \qquad (Eq\ 2.3)$$

As mentioned earlier, the electrical potential of an ISE in a potentiometric cell is measured at equilibrium conditions against a reference electrode (Figure 8).

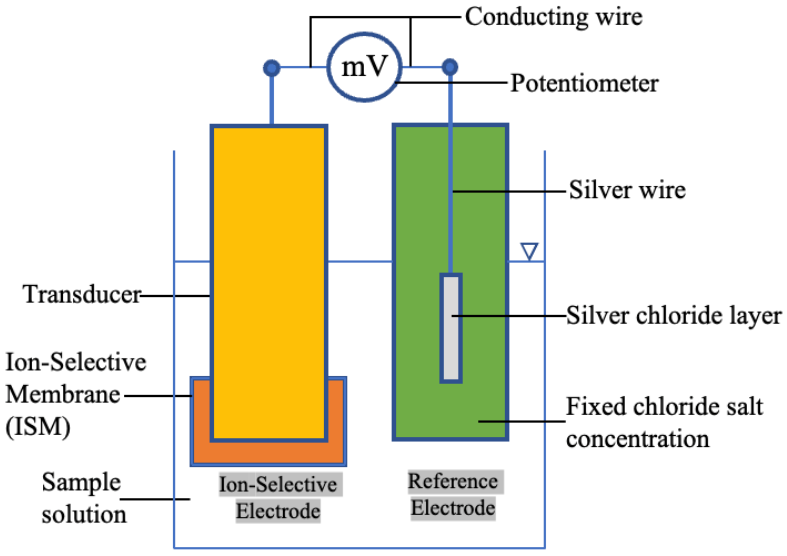

Figure 8. Schematic illustration of a potentiometric measurement setup using solid-state reference and ion-selective electrodes.

It should be noted that ISEs do not respond to ionic concentration, amount per unit volume of sample; rather, they respond to ionic activity. Activity depends on concentration and the

interaction between all ions present in the sample. The interactions quantified by the activity coefficient (γ_i) are related to concentration (C_i) and activity (a_i) of an ion i by the equation below:

$$a_i = \gamma_i \cdot C_i \qquad (Eq\ 2.4)$$

The activity coefficient is derived from the limiting law of the Debye-Hückel theory $(Eq\ 2.5)$[56].

$$log\ \gamma_i = -\frac{A \cdot z_i^2 \cdot \sqrt{J}}{1 + a_{\mathrm{Kjel},i} \cdot B \cdot \sqrt{J}} \qquad (Eq\ 2.5)$$

A and B are constants which depend on the dielectric constant and temperature of the sample. In aqueous samples at 25 °C, A = 0.512 and B = 0.328. The parameters z_i and $a_{\mathrm{Kjel},i}$ are the charge and Kjelland parameter of an ion, i, in the sample. The concentration of all ions in the sample is accounted for by the ionic strength (J) which is calculated using the equation below:

$$J = \frac{1}{2}\sum_{i=1}^{n} C_i \cdot z_i^2 \qquad (Eq\ 2.6)$$

The measured potential during potentiometry is a net sum of all contributing phase boundary potentials. In an ideal potentiometric setup, all potentials are constant except the membrane potential (E_{membrane}) which changes in response to analyte activity in the sample. E_{membrane} is the potential across the ISM | sample interface[19]. The relationship between the net cell potential (E_{cell}) and the analyte activity (a_i) is described by the Nernst equation $(Eq\ 2.7)$. When interfering ions are present in the sample, the overall potential from the Nikolsky-Eisenman equation $(Eq\ 2.8)$ considers their selectivity coefficients with respect to the analyte ($K_{i,j}$)[21].

$$E_{\mathrm{cell}} = E^0 + \frac{2.303 \cdot R \cdot T}{n_i \cdot F} \cdot \log a_i \qquad (Eq\ 2.7)$$

$$E_{\mathrm{cell}} = E^0 + \frac{2.303 \cdot R \cdot T}{n_i \cdot F} \cdot \log(a_i + {a_j}^{z_i/z_j} \cdot K_{i,j}) \qquad (Eq\ 2.8)$$

$$K_{i,j} = 10^{\frac{(E_j - E_i)\cdot z_i \cdot F}{2.303 \cdot R \cdot T}} \cdot \frac{a_i}{{a_j}^{z_i/z_j}} \qquad (Eq\ 2.9)$$

E^0 is the standard potential of the cell which depends on the characteristics of both indicator and reference electrodes. R is the universal gas constant (8.314 J·mol^{-1}·K^{-1}), T is the absolute temperature, and F is the Faraday constant (96 485.33 C·mol^{-1}). The parameters z_i and z_j are the charges of the primary ion (i) and interfering ion (j), respectively. The parameters a_i and a_j are the activities of the primary ion (i) and interfering ion (j), respectively.

The selectivity coefficient, $K_{i,j}$, can be determined using the fixed interference method (FIM), separate solution method (SSM)[21] or matched potential method[57]. $K_{i,j}$ is calculated using the SSM according to equation (Eq 2.9)[58].

Equation (Eq 2.7) mirrors the standard equation of a straight line and is used for determining the slope of the linear part in the calibration curve of an ISE. The Nernstian slope of the linear region in the calibration curve of an ideal monovalent ISE at 25 °C is 59.16 mV/decade for a cationic ISE and −59.16 mV/decade for an anionic ISE (Figure 9). Significant deviations from the Nernstian slope can indicate problems with an ISE. In practice, non-Nernstian slopes are observed due to factors such as components leaching out of the membrane, strongly interfering ions, membrane thickness, and water layer formation[59, 60].

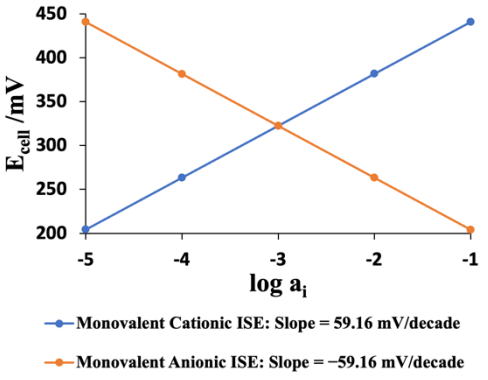

Figure 9. Schematic illustration of the ideal Nernstian response of monovalent ion-selective electrodes.

2.5 Current State of the Flow-Through ISEs

Flow-through analysis allows for continuous measurement of analyte concentrations and can be particularly useful when combined with potentiometric analysis. The short response times of ISEs make them very suitable for rapid and continuous flow-through analysis in different fields such as environmental[61], industrial[62], and clinical[63]. In a flow-through setup, the sample solution is in contact with the reference electrode and one or more ISEs.

A good commercial example is the Thermo Scientific Konelab 20, capable of measuring the concentration of ions such as Na^+, K^+, Cl^-, and Li^+ in biofluids using ISEs[64, 65]. The device can measure volumes as low as 100 µl. However, the measurements are done instrumentally after taking the samples from patients. Such device is not intended for real-time measurements, a gap the work from this thesis aims to narrow. The advantages of a flow-through setup for

microscale sensing have only been slightly explored[49, 66], leaving much room for improvement.

An on-body device which takes advantage of the continuous and fast real-time sensing offered by flow-through ISEs could be very beneficial to different aspects of medicine. Monitoring specific ions such as Na^+, K^+, and Cl^-, in an easily accessible sample like sweat could provide relevant health information such as hydration status and electrolyte balance that can be acted upon by patients immediately. In addition, long-term monitoring could allow for early diagnosis of bigger health issues such as hypertension and cystic fibrosis[67].

2.6 Electrochemical Impedance Spectroscopy

Electrochemical Impedance Spectroscopy (EIS) is an analytical technique used to study the kinetic processes of electrochemical systems. Impedance is a measure of how current flow is restricted in a circuit. A small oscillating signal, typically potential, is applied to the electrochemical cell and the corresponding response, typically current, is measured across a broad range of frequencies. At each frequency point, the sinusoidal response is shifted by a phase angle (φ) from the sinusoidal input. Equations $(Eq\ 2.10)$ and $(Eq\ 2.11)$ show the input and output signals for a galvanostatic EIS, respectively. The impedance (Z) is a ratio of the time-dependent potential (E_t) to the time-dependent current (I_t) $(Eq\ 2.12)$[68].

$$E_t = E_0 \cdot \sin(\omega t) \qquad (Eq\ 2.10)$$

$$I_t = I_0 \cdot \sin(\omega t + \varphi) \qquad (Eq\ 2.11)$$

$$Z = \frac{E_t}{I_t} = Z_0 \cdot \frac{\sin(\omega t)}{\sin(\omega t + \varphi)} \qquad (Eq\ 2.12)$$

When the input potential and current response are expressed as complex functions ($(Eq\ 2.13)$ and $(Eq\ 2.14)$), the impedance (Z) can be seen to consist of a real component (Z') and imaginary component (Z'') $(Eq\ 2.15)$ and $(Eq\ 2.16)$[68].

$$E_t = E_0 \cdot \exp(j\omega t) \qquad (Eq\ 2.13)$$

$$I_t = I_0 \cdot \exp(j\omega t + \varphi) \qquad (Eq\ 2.14)$$

$$Z = Z_0 \cdot \exp(j\varphi) = Z_0 \cdot (cos\varphi + jsin\varphi) \qquad (Eq\ 2.15)$$

$$Z = Z' + j \cdot Z'' \qquad (Eq\ 2.16)$$

Where $j = \sqrt{-1}$ is the imaginary number, E_0 and I_0 are amplitudes of the applied potential and current response, respectively. ω is the radial (or angular) frequency measured in rad/s. Z_0 is the magnitude of the impedance and t is time.

For visual representation of the EIS results, Bode and Nyquist plots are used. Bode plots display the logarithm of the impedance and the phase angle versus the logarithm of the frequency. Nyquist plots display the negative of the imaginary component of the impedance, $-Z''$, versus the real component of the impedance, Z'. For studying the resistance of ISMs, the Nyquist plots are typically used as they can easily be correlated to Randles equivalent circuits (Figure 10). A Randles equivalent circuit uses electrical components such as resistors and capacitors to model the electrochemical processes in a system[69].

An ideal ISM can be modelled with an ideal Randles circuit (Figure 10)[69, 70], where the solution resistance (R_s) is often negligible compared to the other elements of the equivalent circuit[71]. R_{ct} corresponds to the width of the semicircle and represents the charge transfer resistance of the membrane. C_{dl} is the double-layer capacitance and Z_W is the Warburg impedance which describes diffusion, signal transduction, and other slower processes observed at low-frequency ranges[69].

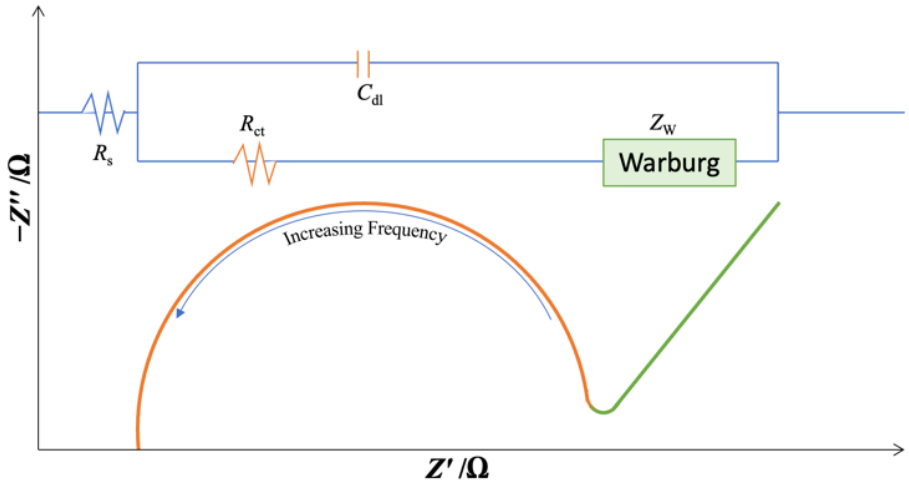

Figure 10. Schematic representation of the ideal Nyquist plot of an ISM and the corresponding Randles equivalent circuit.

3 Experimental

3.1 Chemicals and Materials

AgCl-saturated 3 M KCl solution was purchased from Mettler Toledo. Lithium acetate dihydrate ($LiOAc{\cdot}2H_2O$, 98%) was purchased from Acros Organics. Polyvinyl butyral (PVB), tetrahydrofuran (THF, ≥99.5%), methanol (≥99%), vinyl acetate monomer (VAc, ≥99%), photo-initiator 2,2-dimethoxy-2-phenylacetophenone (DMPP, 99%), multiwalled carbon nanotube (MWCNT, carbon >95%), potassium chloride (KCl, ≥99.0%), Ag/AgCl (60/40) paste for screen printing, high molecular weight polyvinyl chloride (PVC), potassium ionophore I (valinomycin), potassium tetrakis[3,5-bis(trifluoromethyl)-phenyl]borate (KTFPB), bis(2-ethylhexyl) sebacate (DOS, ≥97%), 2-nitrophenyl octyl ether (oNPOE, 99%), sodium bicarbonate ($NaHCO_3$, ≥99.5%), and L-(+)-lactic acid lithium salt ($C_3H_5LiO_3$, 97%) were purchased from Sigma-Aldrich. Polyvinyl acetate (PVAc) powder was obtained from Wacker (Vinnapas B60 Finely ground). Sodium chloride (NaCl, ≥99.5%) and magnesium chloride hexahydrate ($MgCl_2{\cdot}6H_2O$, ≥99.5%) were purchased from Merck. Calcium chloride dihydrate ($CaCl_2{\cdot}2H_2O$, ≥99%) and tridodecylmethylammonium chloride (TDMAC, 98%) were purchased from Fluka Chemicals. Carbon cloth (CC) (Kynol® activated carbon fabric ACC-5092–20) was purchased from Kynol Europa. Gold wire (24 carats, 1 mm diameter) was purchased from City Gold, Turku. Polycarbonate (PC) sheet was purchased from ETRA Oy. Silver wire (99.99%, 1 mm diameter) was purchased from Kultajousi, Turku. Ultrapure water (ELGA, 18.2 MΩ cm) was used to prepare all aqueous solutions.

3.2 Instrumentation

The galvanostatic chlorination was done using a Metrohm Type E 211 coulometer.

Potentiometric measurements were done using a 16-channel high input impedance potentiometer (10^{15} Ω, Lawson Laboratories) and EMF Suite 2 software. A commercial double-junction Ag/AgCl/3 M KCl reference electrode (6.0726.100 Metrohm) with 1 M lithium acetate (LiOAc) outer filling solution was used in the potentiometric measurements. A commercial solid-state chloride-ion-selective electrode (Orion 9417BN, Thermo Scientific) was used in the potentiometric measurements as an external ion-selective electrode.

Chemical polymerisation was done with a UV lamp (NAIL-EON), delivering 36 watts of UV (365 nm) light.

A peristaltic pump (FIAlab Instruments, Alitea AB) was used to pump the samples during flow-through measurements.

Electrochemical Impedance Spectra (EIS) measurements were done in a three-electrode set-up using Autolab General Purpose Electrochemical System (AUT20.FRA2-Autolab, Eco Chemie) and the Autolab Frequency Response Analyzer (FRA) software. A Metrohm single junction Ag/AgCl/3 M KCl reference electrode (6.0733.100, Metrohm) was used in the EIS measurements.

The measuring cells, made from polycarbonate (PC) sheets, were 40 mm wide with a 20 mm diameter cavity for holding the CC-based electrodes. The single-cell PC supports had a ~1.5 mm deep cavity, and the double-cell PC support had a ~4 mm deep cavity. The PC supports had a 2.5 mm wide flow-through channel in the middle and openings on the top cover for the gold wire conductors. The separator used in the double-cell PC support was made of Teflon and was ~1 mm thick. Figure 11 shows pictures of the single-cell PC support and the double-cell PC support with the Teflon separator.

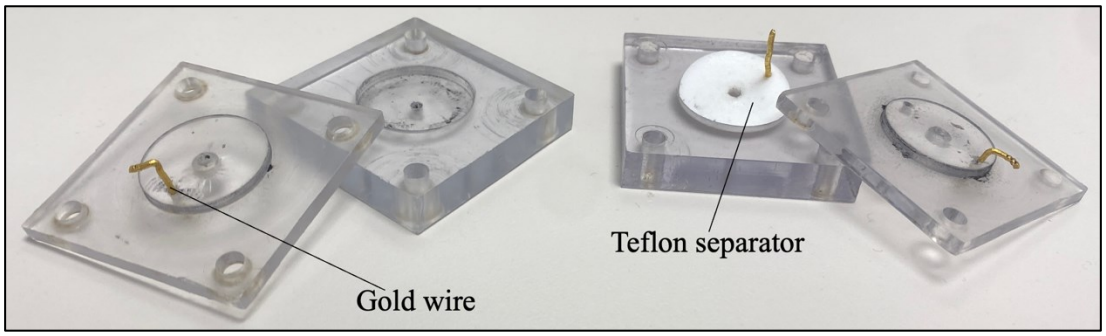

Figure 11. Left: Single-cell polycarbonate support. Right: Double-cell polycarbonate support with Teflon separator.

3.3 Testing Reference Electrode Designs

To evaluate the performance of two potential solid-state reference electrode designs to be used in the flow-through cell, the designs were first tested using 3 mm diameter silver disk electrodes mounted in PVC cylinders. To deposit a silver chloride layer, the silver electrode was chlorinated galvanostatically using 1 M KCl solution and by passing a current of 0.1 mA for

30 minutes. Using the prepared Ag/AgCl electrodes, three different types of reference electrodes were made as described below:

3.3.1 Ag/AgCl with PVB/NaCl Layer

The PVB/NaCl membrane cocktail used here and for other parts of this thesis was prepared by adding 5 ml of methanol to 0.4 g of PVB and 0.25 g of NaCl in a vial. The cocktail was vortexed for 1 minute at 2500 rpm and ultrasonicated for 1 hour.

A 100 µl volume of the PVB/NaCl membrane cocktail was drop cast on one Ag/AgCl electrode and allowed to dry overnight. After drying, the electrode was conditioned and stored in 0.1 M KCl solution. This electrode will be referred to as **DE1** (Disk Electrode 1) henceforth.

On another Ag/AgCl electrode, 200 µl of the PVB/NaCl cocktail was drop cast in two 100 µl portions with a 2-hour drying time between the two additions. The electrode was allowed to fully dry overnight, then conditioned and stored in 0.1 M KCl solution. This electrode will be referred to as **DE2**.

3.3.2 Ag/AgCl with MWCNTs & PVB/NaCl Layers

A mixture, containing 0.005 g of MWCNTs dissolved in 1 ml THF, was prepared and vortexed for 1 minute at 2500 rpm and then ultrasonicated for 2 hours. A 100 µl volume of the mixture was drop cast on two Ag/AgCl electrodes, prepared as described in 3.3, in two 50 µl portions with a 30-minute drying time between the two additions. The resulting Ag/AgCl/MWCNTs electrodes were left to dry overnight.

A 100 µl volume of the PVB/NaCl membrane cocktail was drop cast on one Ag/AgCl/MWCNTs electrode and allowed to dry overnight. After drying, the electrode was conditioned and stored in 0.1 M KCl solution. This electrode will be referred to as **DE3** henceforth.

On the other Ag/AgCl/MWCNTs electrode, 200 µl of the PVB/NaCl cocktail was drop cast in two 100 µl portions with a 2-hour drying time between the two additions. The electrode was allowed to fully dry overnight, then conditioned and stored in 0.1 M KCl solution. This electrode will be referred to as **DE4**.

3.3.3 Ag/AgCl with Polyvinyl Acetate/KCl Layer

A mixture for making the PVAc/KCl composite used here and for other parts in this thesis, was prepared using the following composition in %(w/w): 49.5 KCl, 0.5 DMPP, 20 PVAc, and

30 VAc. The KCl used in making the composite was first dried at 500 ℃ then ground using a mortar and pestle to have as fine of a powder as possible. The components were mixed in a glass vial, vortexed for 1 minute at 2500 rpm, covered with aluminium foil, and placed on a nutating mixer overnight.

A transfer pipette was used to drop cast the mixture onto one Ag/AgCl electrode prepared as described in 3.3. Drop casting could not be easily measured volumetrically due to the viscosity of the mixture, but enough volume of the mixture was added to form a spherical membrane on the electrode surface. To prepare the PVAc/KCl composite, polymerisation was done under UV light for 10 minutes. The electrode was then conditioned and stored in 0.1 M KCl solution. This electrode will be referred to as **DE5** for the rest of this text.

3.4 Fabricating Planar Solid-State Composite Reference Electrodes

Two designs for preparing planar solid-state PVAc/KCl composite-based reference electrodes were studied in this work:

3.4.1 PVAc/KCl Composite-Based Planar Reference Electrode using CC Substrate (CC-RE)

A 20 mm diameter piece of carbon cloth (CC) was cut, and a 4 mm hole was punched in the middle of it using a hole punching tool. The carbon cloth was placed on a polytetrafluoroethylene (PTFE) support. Ag/AgCl paste was brushed in the hole and slightly in the area around the hole. The Ag/AgCl paste was brushed on three times with 15 minutes of drying in between using an 80 ℃ oven. After the third brushing, the drying was done for 30 minutes at 80℃. The carbon cloth was then flipped to the back, and the Ag/AgCl paste was brushed once in the middle and in a small area around the hole. Finally, the electrode was allowed to dry for 30 minutes at 80 ℃.

After complete drying of the Ag/AgCl paste, the mixture used for preparing the PVAc/KCl composite was added on the Ag/AgCl paste layer using a spatula and the chemical polymerisation was done using UV light for 5 minutes on one side of the carbon cloth. The mixture was then spread on the other side of the carbon cloth and polymerised under UV light for 5 more minutes. The mixture was spread to cover the entire Ag/AgCl paste layer. The initial polymerisation time was short enough to ensure that the composite layer was soft enough to punch a hole through. A 2.5 mm hole was punched through the middle of the composite layer and the polymerisation was continued for 10 more minutes on each side to harden the

composite layer. The electrode was then conditioned in 0.1 M KCl. This electrode will be referred to as **CC-RE** for the rest of this text. Figure 12 shows a schematic illustration of the CC-RE.

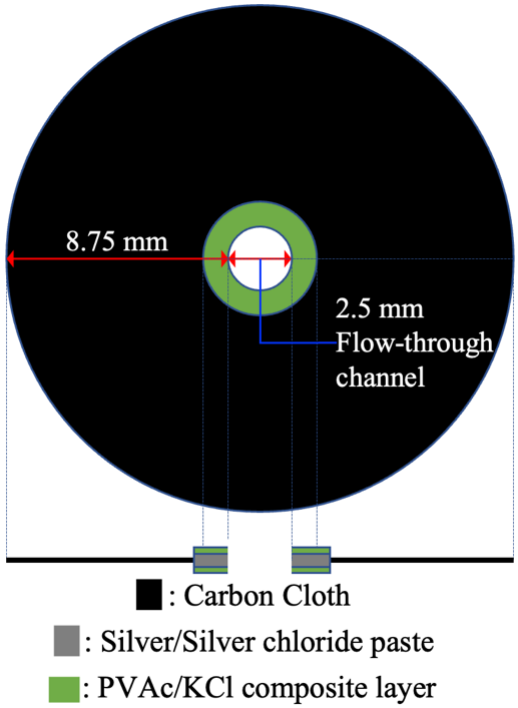

Figure 12. Schematic illustration of the PVAc/KCl composite-based planar reference electrode made using CC substrate (top and side views).

3.4.2 PVAc/KCl Composite-Based Planar Reference Electrode using PC Support (PC-RE)

The electrode for this design was made using the lower part of the single-cell PC support without its top cover (Figure 11). A silver wire was bent into a spiral to fit into the cell, and an Ag/AgCl layer was galvanostatically chlorinated on the spiral region. Chlorination was done using 1 M KCl solution and by passing a 0.1 mA current for 1 hour.

After chlorination, the wire was dried and placed in the cell. A layer of the mixture, used for preparing the PVAc/KCl composite, was spread on the wire to fill the cavity of the cell. Part of the silver wire (without an AgCl layer) was left exposed for connecting to the potentiometer. The cell was placed under UV light for 30 minutes to polymerise the composite mixture. After polymerisation, the electrode was conditioned in 0.1 M KCl overnight. After conditioning, a sharp piercing tool was used to make a hole through the middle of the composite. This hole was made after conditioning because water uptake softened the composite layer. The electrode

was stored in 0.1 M KCl between measurements. This electrode will be referred to as **PC-RE** for the rest of this text. Figure 13 shows a schematic illustration of the PC-RE, and Figure 14 shows a picture of different stages in its manufacturing process.

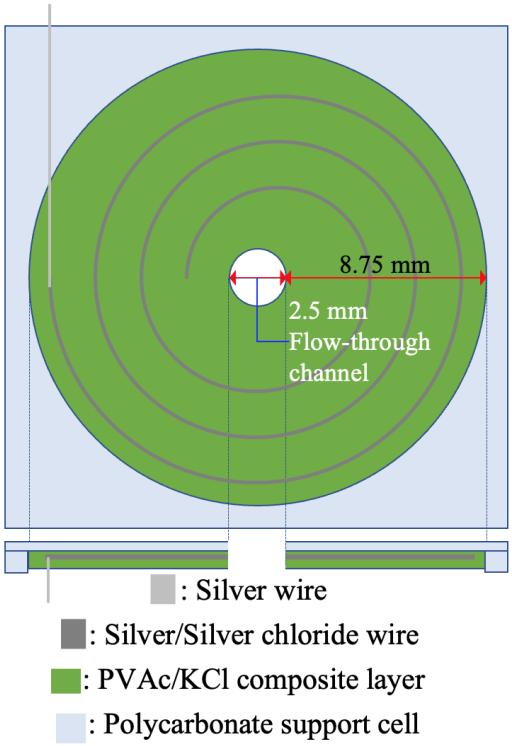

Figure 13. Schematic illustration of the PVAc/KCl composite-based planar reference electrode made using PC support (top and side views).

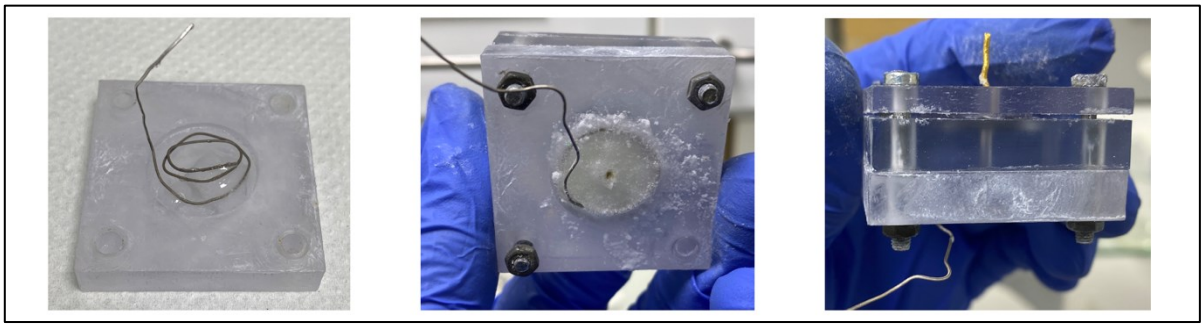

Figure 14. Manufacturing process of the PVAc/KCl composite-based planar reference electrode made using PC support. From left to right: spiral Ag/AgCl wire and the mixture for making the PVAc/KCl composite inside the support; the electrode after polymerisation under UV light for 30 minutes, overnight conditioning in 0.1 M KCl and piercing the flow-through hole; combination of the reference electrode (bottom) with the cell containing an ISE (top).

3.5 Fabrication of Ion-Selective Electrodes

The carbon cloth-based ion-selective electrodes (CC-ISEs) were all made using a 20 mm diameter piece of carbon cloth with a 4 mm hole punched in the middle. The carbon cloth pieces were placed on a PTFE support during drop casting of the ion-selective membrane cocktail.

3.5.1 Potassium Ion-Selective Electrodes (K-ISEs)

The composition of the potassium ion-selective membrane (K-ISM) cocktail, in %(w/w), was: 1.0 valinomycin, 0.5 KTFPB, 65.2 DOS, and 33.3 PVC dissolved in THF (dry mass is 20%). The components were mixed in a vial, vortexed for 1 minute at 2500 rpm, covered with aluminium foil, and placed on a nutating mixer overnight.

A 100 µl volume of the K-ISM cocktail was drop cast on the area around the 4 mm hole in the carbon cloth piece and left to dry for 45 minutes. After drying, compressed air was blown through the middle of the hole to remove loose carbon cloth fibres. The membrane cocktail was drop cast into the 4 mm hole in five 50 µl portions with a 45-minute drying time between each addition. After the fifth drop casting step, the membrane was left to dry for 4 hours. The carbon cloth was flipped to the back and a 75 µl volume of the cocktail was added in the middle of the carbon cloth while ensuring some of it spread just outside the area around the hole and the electrode was left to dry. Four identical K-ISEs, **K0**, **K1**, **K2**, and **K3** were made.

3.5.2 Chloride Ion-Selective Electrodes (Cl-ISEs)

The composition of the chloride ion-selective membrane (Cl-ISM) cocktail, in %(w/w), was: 15 TDMAC, 51 oNPOE, and 34 PVC dissolved in THF (dry mass is 20%). The components were mixed in a vial, vortexed for 1 minute at 2500 rpm, covered with aluminium foil, and placed on a nutating mixer overnight.

A 50 µl volume of the Cl-ISM cocktail was drop cast on the area around the 4 mm hole of the carbon cloth piece and left to dry for 45 minutes. After drying, compressed air was blown through the middle of the hole to remove loose carbon cloth fibres. The membrane cocktail was drop cast into the hole in four 50 µl portions with a 45-minute drying time between each addition. After the fourth drop casting step, the membrane was left to dry for 4 hours. The carbon cloth was flipped to the back and another 50 µl of the cocktail was added in the middle of the carbon cloth while ensuring some of it spread just outside the area around the hole and the electrode was then left to dry. Three identical electrodes, **Cl1**, **Cl2**, and **Cl3** were made.

Figure 15 shows a schematic illustration of the ISE design, and Figure 16 shows a picture of different stages in the manufacturing process.

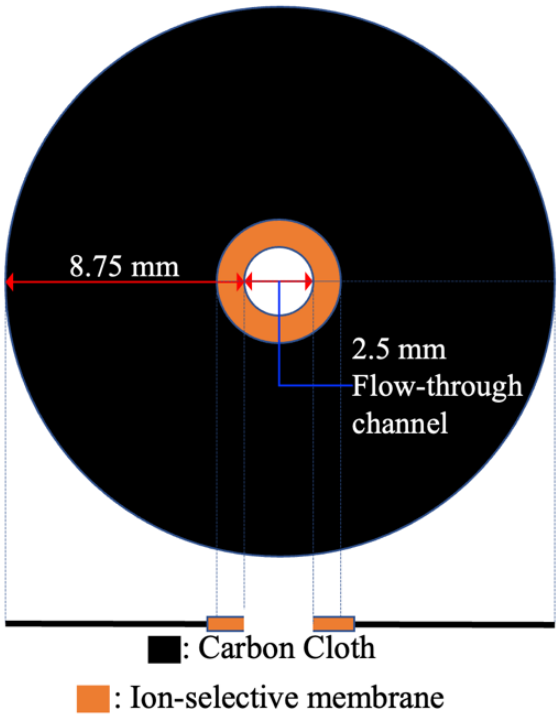

Figure 15. Schematic illustration of the ion-selective electrodes (top and side views).

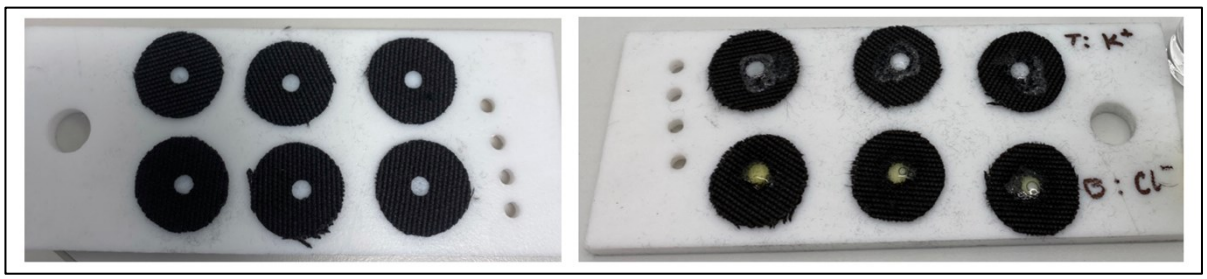

Figure 16. Manufacturing process of the ISEs. From left to right: 20 mm diameter carbon cloth with 4 mm diameter hole before drop casting of the ISM cocktail; the ISEs after drop casting of the ISM cocktail.

3.6 Summary of the Prepared Electrodes

The table below provides a summary of the reference electrodes and ISEs prepared and studied in this thesis.

Table 2. Different reference electrodes and ISEs designed in this thesis.

Electrode(s)	Design	Section
Disk Reference Electrodes		
DE1, DE2	Ag/AgCl disk electrodes with PVB/NaCl membrane	3.3.1
DE3, DE4	Ag/AgCl/MWCNTs disk electrodes with PVB/NaCl membrane	3.3.2
DE5	Ag/AgCl disk electrode with PVAc/KCl composite	3.3.3
Planar Reference Electrodes		
CC-RE	Ag/AgCl paste with PVAc/KCl composite on CC substrate	3.4.1
PC-RE	Ag/AgCl wire with PVAc/KCl composite on PC support	3.4.2
CC-ISEs		
K0, K1, K2, K3	K-ISEs	3.5.1
Cl1, Cl2, Cl3	Cl-ISEs	3.5.2

3.7 Potentiometric Measurements

Two different potentiometric measurement setups were used in this work.

3.7.1 Setup using an External Electrode

In this setup, a CC-based electrode (CC-RE or CC-ISE) was put into the single-cell PC support (Figure 11) and screwed close. A syringe with parafilm around the tip was connected to the hole on top of the cell to hold the solution being measured. A pipette tip covered with parafilm was placed at the bottom of the cell to stop the sample from flowing out the cell. The potentiometric measurements carried out using this setup were done using external electrodes. A commercial double junction (Ag/AgCl/3 M KCl/1 M LiOAc) reference electrode was used

to study the CC-ISEs, (Figure 17a), and a commercial chloride ion-selective electrode was used to study the performance of the CC-RE (Figure 17b). A gold wire in contact with the carbon cloth in the PC support was used to connect the electrode to the potentiometer either as the indicator or as the reference electrode.

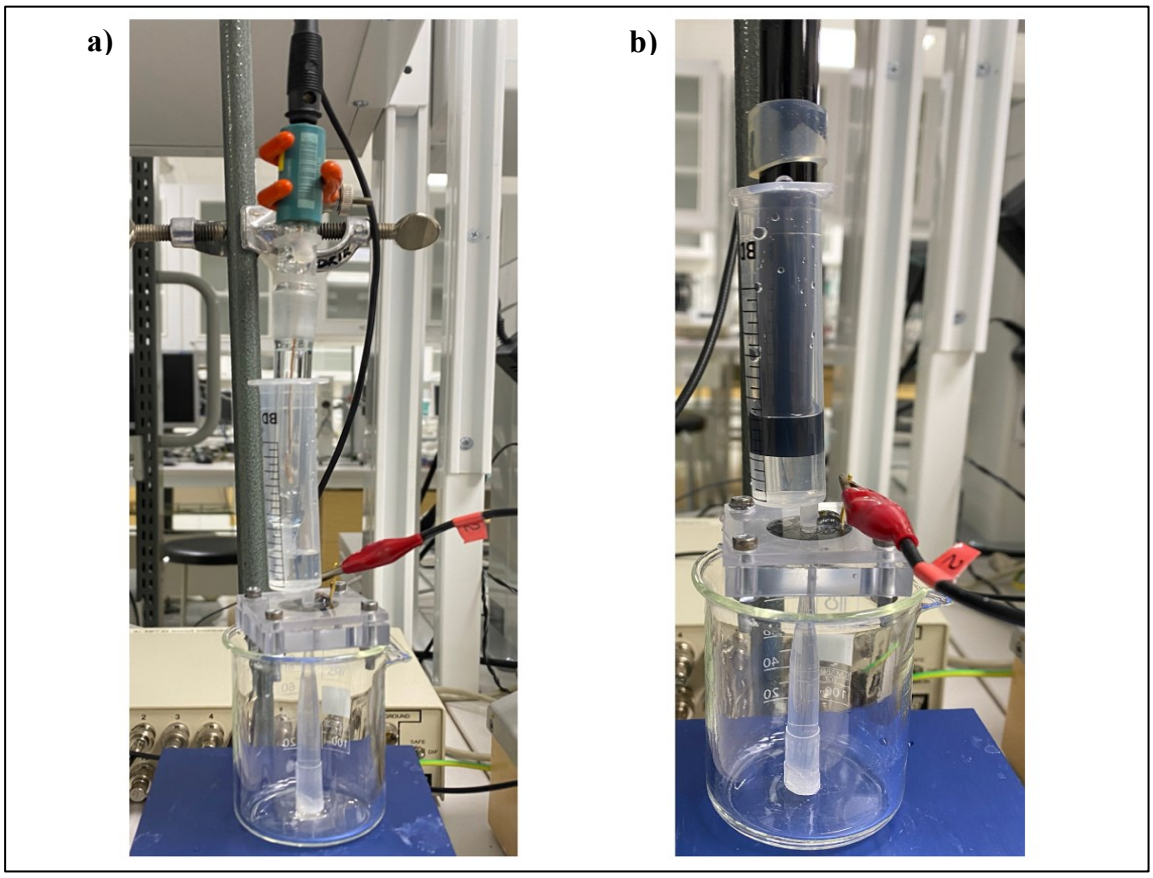

Figure 17. Images of the potentiometric setups with an external electrode. a) Setup with a commercial Ag/AgCl double junction reference electrode b) Setup with a commercial chloride ion-selective electrode.

3.7.2 Flow-Through Setup

This setup was used to measure the response of one or two CC-ISEs against a prepared planar reference electrode.

When used with the CC-RE, one CC-ISE was measured at a time because the double-cell was too small to fit more than one CC-ISE with the CC-RE. The CC-ISE and CC-RE were placed in a double-cell PC support with a Teflon separator between them and screwed shut. The CC-RE was placed at the bottom, and the CC-ISE at the top. Both electrodes were connected to the potentiometer via gold wires. A piece from the carbon cloth of the electrode on the top was cut to avoid contact with the gold wire from the bottom electrode (Figure 18).

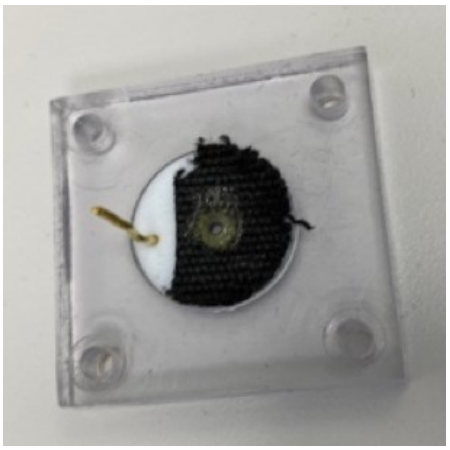

Figure 18. Piece of carbon cloth cut from the top CC-ISE to avoid contact with the gold wire connected to the other CC-based electrode at the bottom.

When used with the PC-RE, one or two CC-ISEs could be measured at a time. The PC-RE was in a separate measurement cell from the CC-ISE(s). Because the measured solution flowed from top to bottom, the PC-RE was kept at the bottom to avoid contamination of the CC-ISEs from the PC-RE. When only one ISE was being used, it was put in the single-cell PC support. When two ISEs were being used in a double-cell PC support, a Teflon separator was placed between them, and the top CC-ISE was cut to avoid contact with the gold wire from the bottom CC-ISE (Figure 18). For measurements with a K-ISE and Cl-ISE, the Cl-ISE was cut and used as the top ISE. Gold wires were used to connect the CC-ISEs to the potentiometer, and the PC-RE was connected via its silver wire. The flow-through channels of the PC-RE and CC-ISE cells were aligned, and the cells were screwed together for measurement (Figure 19). The flow rate of the solution during flow-through measurements was approximately 0.5 ml/min.

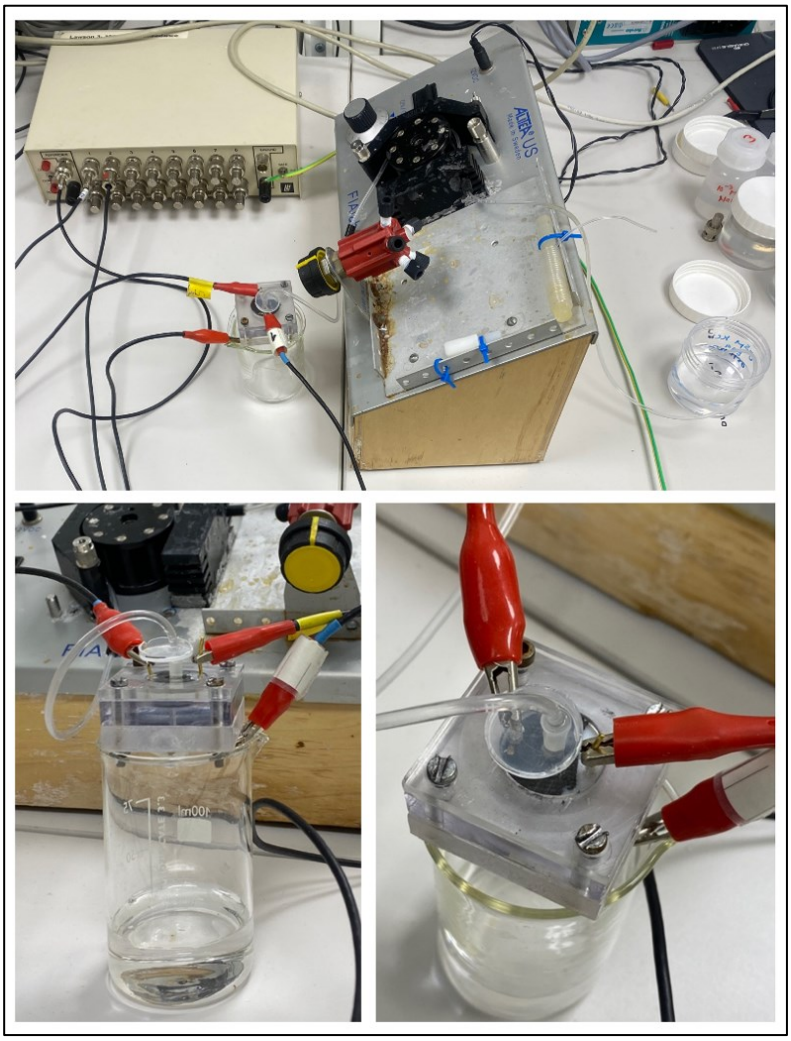

Figure 19. Images of the flow-through potentiometric setup with two CC-ISEs connected via gold wires to the potentiometer and the PC-RE, at the bottom, connected via silver wire.

3.7.3 Calibration Curves

For making the calibration curves, measurement in each solution concentration was done for at least 5 minutes until a stable potential was reached. In a calibration curve, the potentials plotted against the activities of the measured ion were the average of the last five potential values at each concentration. Unless stated otherwise, the displayed linear regression values (slope and intercept/standard potential) were calculated from the 10^{-3} M to 10^{-1} M linear range of the calibration curve. Unless stated otherwise, measurements were done in order of low to high concentrations.

The activity coefficients used to calculate the activity of the ions were obtained according to the Debye-Hückel theory $(Eq\ 2.5)$[56, 72].

3.7.4 Selectivity Coefficient Determination

The selectivity coefficient of one of the K-ISEs, K1, to potassium ion was determined in the presence of three cations (Na^+, Ca^{2+}, and Mg^{2+}). Similarly, the selectivity coefficient of one of the Cl-ISEs, Cl2, to chloride ion was determined in the presence of two anions (bicarbonate [HCO_3^-] and lactate [$C_3H_5O_3^-$]). These ions were selected due to their significant presence in sweat[6]. Chloride salts of the cations, sodium bicarbonate and lithium lactate were used to prepare the respective solutions of the interfering ions. The selectivity coefficients were calculated using the SSM ($Eq\ 2.9$)[58]. The activity coefficients used to calculate the activity of the ions were obtained according to the Debye-Hückel theory ($Eq\ 2.5$)[56, 72]. The CC-ISEs were measured against the PC-RE using the flow-through setup. Between each solution, ultrapure water flowed through the setup for 5 minutes.

3.8 Electrochemical Impedance Spectroscopy Measurement

The EIS measurements were performed to evaluate and compare the resistance of the plasticized PVC-based ISMs in the fabricated K-ISEs. These measurements were done using electrodes K1, K2, and K3 (one at a time) in an external electrode setup (3.7.1). Nitrogen gas was bubbled through 0.1 M KCl solution for 10 minutes and the deaerated solution was used as the electrolyte that was placed in the syringe. The CC-ISE being measured was put in a single-cell PC support and connected as the working electrode. The Ag/AgCl/3 M KCl commercial reference electrode and a glassy carbon rod were placed in the 0.1 M KCl solution and connected as the reference and counter electrode, respectively. The measurements were performed at open-circuit potential using 100 mV excitation amplitude in the 100 kHz to 10 mHz frequency range.

4 Results and Discussion

4.1 Disk Reference Electrodes

The performance of different reference electrodes prepared in this work was first studied and evaluated in order to choose the best option for use in the flow-through potentiometric cell. The responses of solid-state reference electrodes made using Ag/AgCl disk electrodes, DE1 to DE5, were measured for 800 s in 0.1 M KCl solution using a commercial double-junction reference electrode. The responses were recorded after 36 hours of conditioning the electrodes in 0.1 M KCl solution. As can be seen in Figure 20, the PVB/NaCl-based reference electrodes with the thicker membrane, DE2 and DE4, had the most significant potential deviation from the 0 mV value. Whereas, the potentials measured for other PVB/NaCl-based reference electrodes with thinner membranes, DE1 and DE3, showed less potential deviation from the 0 mV value compared to DE2 and DE4. The best option was the PVAc/KCl composite-based reference electrode, DE5, which showed the least potential deviation (ca. –4 mV) from 0 mV.

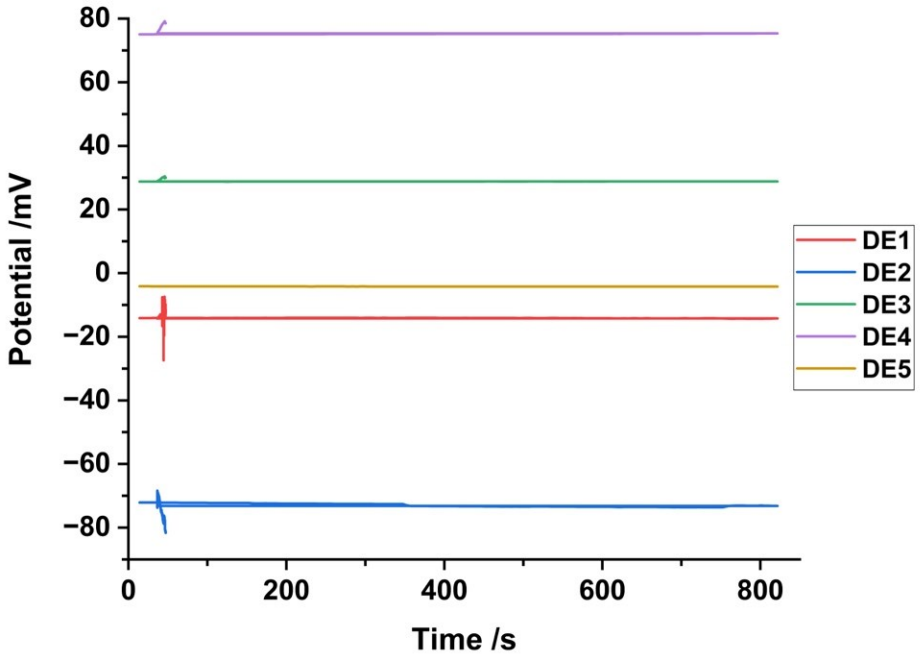

Figure 20. Time-dependent response of five conditioned solid-state reference Ag/AgCl electrodes made using Ag/AgCl silver disk electrodes in a PVC body and measured against a commercial double-junction reference electrode in 0.1 M KCl solution.

After conditioning, each of the electrodes, DE1 to DE5, was used as reference electrodes in the calibration of a commercial chloride ISE in 10^{-3} M to 10^{-1} M KCl solutions. The calibration curves, as well as the slope and standard potential (E^0) values calculated from the linear range 10^{-3} M to 10^{-1} M KCl, are displayed in Figure 21. The reference electrodes, DE3 and DE4, with a MWCNTs layer between the Ag/AgCl substrate and the PVB/NaCl membrane, resulted in super-Nernstian slopes for the calibration curves. This result is contrary to the results from a previous work in which the electrode with a CNT layer between the Ag/AgCl layer and the PVB/NaCl membrane showed better response than the electrode without the CNT layer[52]. The reason for the super-Nernstian response was not further investigated experimentally in this thesis. However, one hypothesis for the observed super-Nernstian response is that the adsorption of ions on the MWCNTs resulted in an increased junction potential at the reference electrode.

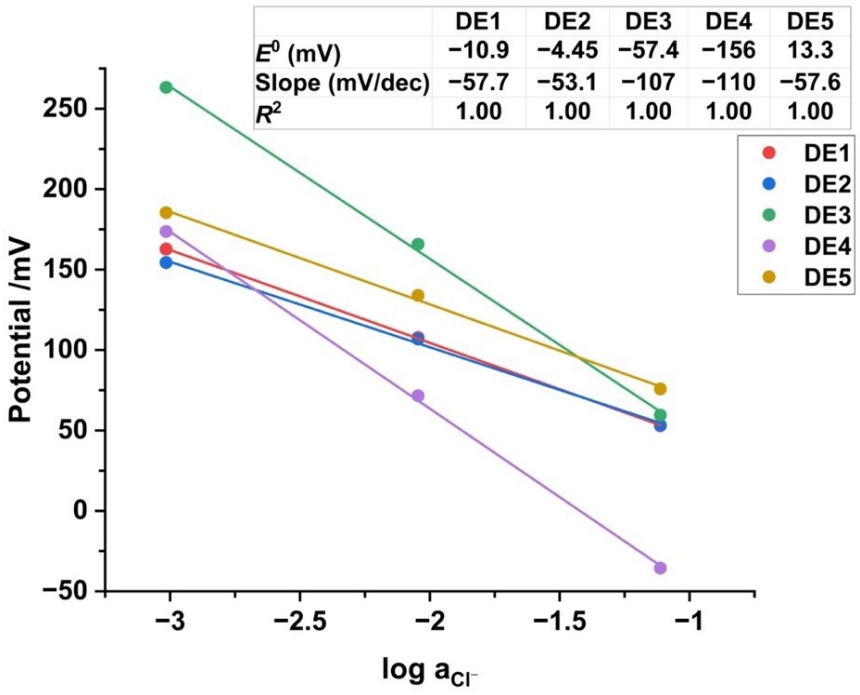

Figure 21. The curves obtained from calibrating a commercial solid-state chloride ISE against each of the solid-state reference electrodes, DE1 to DE5, in 10^{-3} M to 10^{-1} M KCl solutions.

Due to lower deviation in the potential of the PVAc/KCl composite-based reference electrode (DE5) from the 0 mV value when compared against the Ag/AgCl commercial reference electrode (Figure 20), good performance when used in the calibration of a commercial chloride ISE (Figure 21), and previously demonstrated excellent performance of the composite-based

reference electrodes[14, 15], the PVAc/KCl composite-based option was selected for preparing planar reference electrodes used in this work.

4.2 Calibration of CC-ISEs against a Commercial Reference Electrode

Before using the CC-ISEs for measurements in the flow-through setup, one K-ISE, K1, and one Cl-ISE, Cl2, were calibrated against a commercial double-junction reference electrode (Ag/AgCl/3 M KCl/1 M LiOAc) using the external electrode setup (3.7.1). The measurements were done to verify that the batch of CC-ISEs exhibited a typical and acceptable response. Figure 22 shows the result from the calibration of K1 and Cl2 in 10^{-3} M to 10^{-1} M KCl solutions. Both electrodes showed a linear response in this concentration range with near-Nernstian slopes. The observed responses indicated proper functioning of the CC-ISEs.

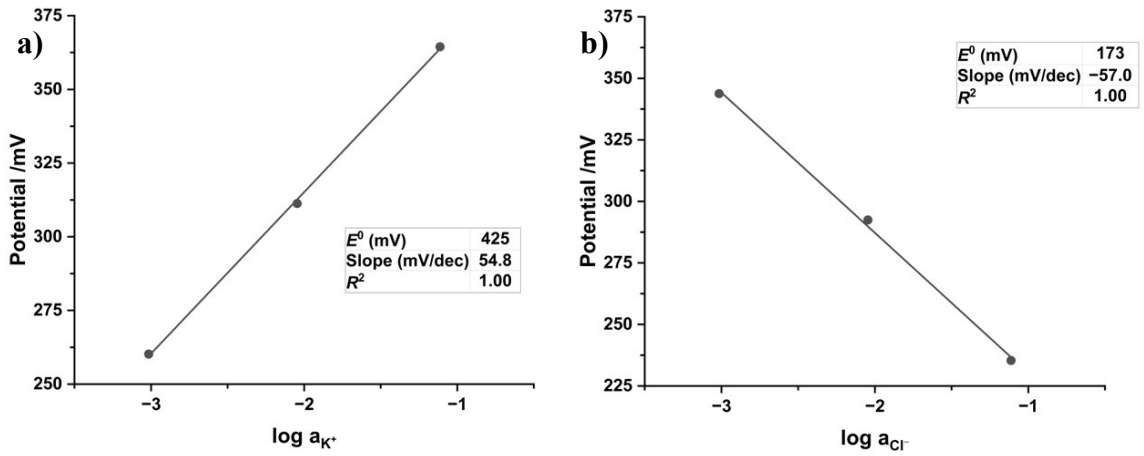

Figure 22. Calibration curves of CC-ISEs (a: K1; b: Cl2) in 10^{-3} M to 10^{-1} M KCl solutions against a commercial double-junction reference electrode using the external electrode setup.

4.3 PVAc/KCl Composite-Based Planar Reference Electrode using CC Substrate (CC-RE)

4.3.1 CC-RE vs. Commercial Reference Electrode

The first attempt for making a planar solid-state PVAc/KCl composite-based reference electrode for the flow-through cell used carbon cloth as substrate (3.4.1). After making the electrode, it was conditioned in 0.1 M KCl while the potentiometric response was monitored versus a commercial double-junction reference electrode using the external-electrode setup. Figure 23 shows that the electrode approached a potential of ca. –8 mV, indicating a good resemblance to the commercial reference electrode. Moreover, the electrode demonstrated a

reasonably short conditioning time with its potential approaching stability in ca. 6 hours after first contact with the conditioning solution.

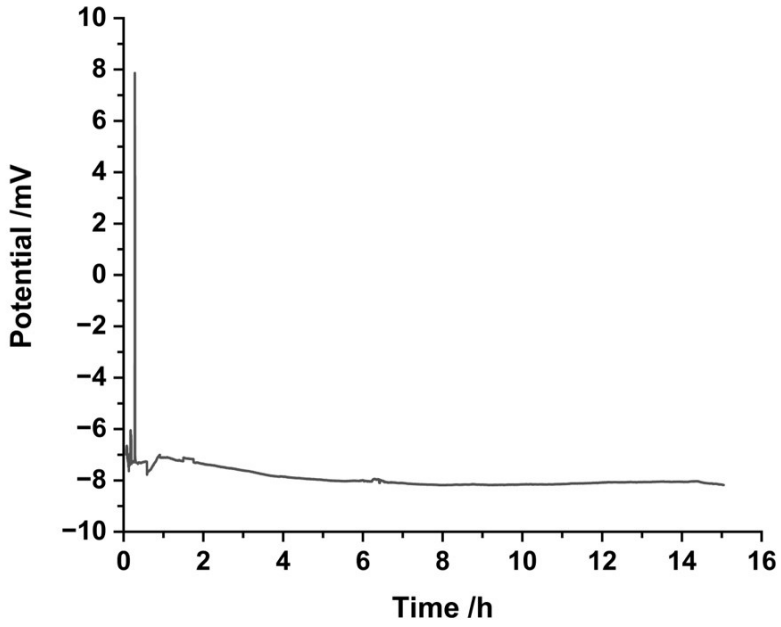

Figure 23. Initial conditioning response of the CC-RE in 10^{-1} M KCl solution measured against a commercial reference electrode using the external electrode setup.

An important property of a reference electrode is the potential stability in solutions with varying chloride concentrations. A stable potential in solutions of different chloride concentration shows that the chloride salt containing layer, in the structure of the reference electrode, is able to maintain constant chloride concentration at the Ag/AgCl layer and the reference electrode does not respond to chloride ions in the sample.

The potential of the conditioned CC-RE was measured against a commercial reference electrode in 10^{-1} M and 10^{-4} M KCl solutions using the external electrode setup. In the *regular* setup, the commercial reference electrode was connected to the reference channel of the potentiometer and the CC-RE was connected to one of the indicator electrode channels. In the *reverse* setup, the connections were reversed, i.e., the CC-RE was connected to the reference channel and the commercial reference electrode to one of the indicator channels. For both the *regular* and *reverse* setups, Figure 24 shows an acceptable <2mV potential difference across a 3-decade concentration difference. In addition, Figure 24 shows that the responses of the *regular* and *reverse* setups almost mirror each other, i.e., the measured potentials are close to each other but differ by sign.

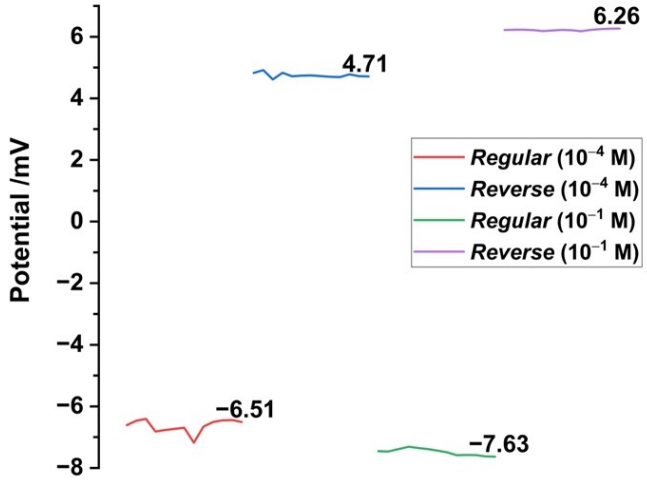

Figure 24. The potential response of the CC-RE measured against a commercial double-junction reference electrode (*regular* setup), and the potential response of a commercial double-junction reference electrode measured against the CC-RE (*reverse* setup).

4.3.2 Commercial Chloride ISE vs. CC-RE

After conditioning and comparing the performance of the CC-RE to a commercial reference electrode, it was used in the calibration of a commercial chloride ISE in 10^{-4} M to 10^{-1} M KCl solutions, using the external electrode setup. The result in Figure 25, shows a near-Nernstian response of –54.6 mV/decade for the chloride ISE in the linear range of 10^{-3} M to 10^{-1} M KCl, further demonstrating the suitability of the CC-RE as a reliable reference electrode.

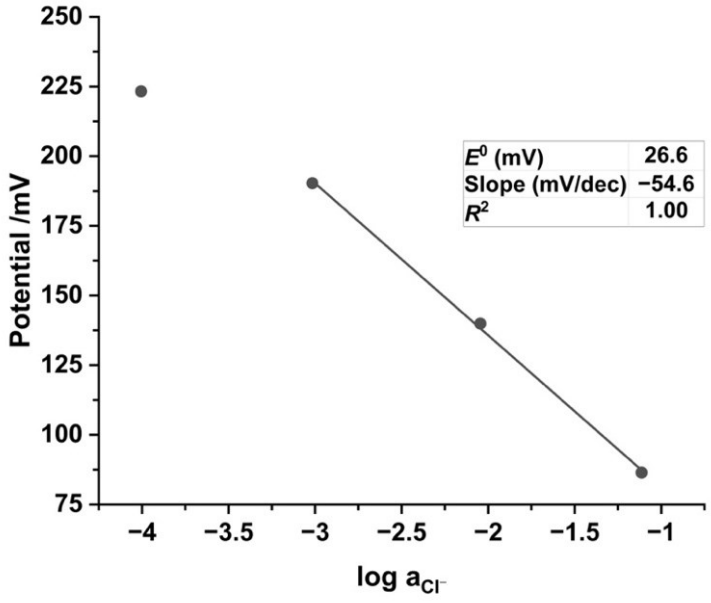

Figure 25. Calibration curve of a commercial chloride ISE measured against the CC-RE in an external electrode setup using 10^{-4} M to 10^{-1} M KCl solutions.

4.3.3 CC-ISE vs. CC-RE

The CC-RE was combined with a potassium CC-ISE (K0) in a double-cell flow-through setup (3.7.2). Figure 26 shows the calibration curves for K0 obtained from two measurements carried out in 10^{-3} M to 10^{-1} M KCl solutions. Measurement 2 was done after Measurement 1 on the same day. Between both measurements it was observed that the composite layer of the CC-RE was significantly compressed by the cell resulting in a much narrower channel. Therefore, before Measurement 2, a new channel was made in the CC-RE to allow for continued flow of solutions through the setup.

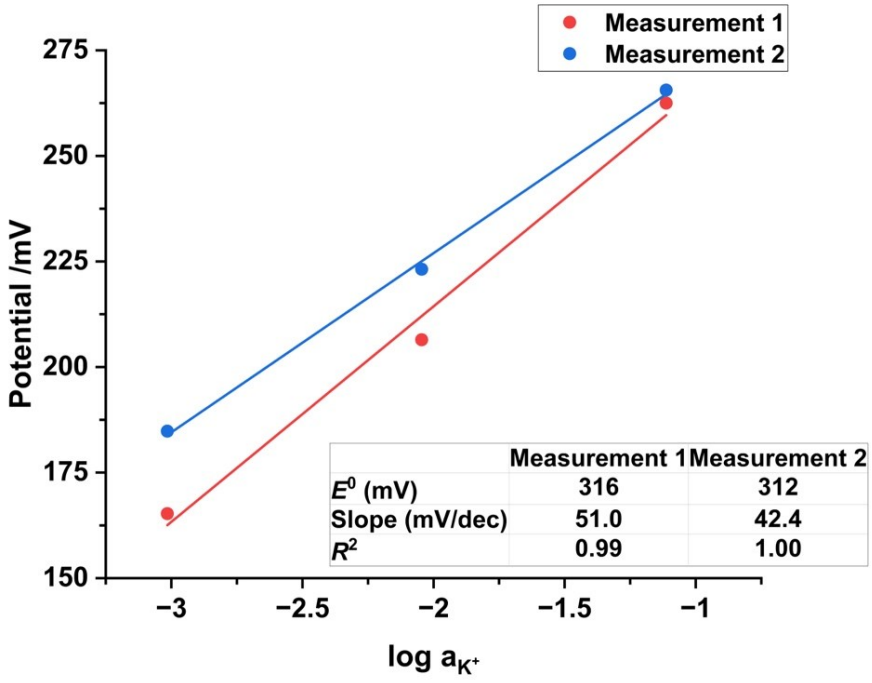

Figure 26. Calibration curves obtained for measurement of a potassium CC-ISE (K0) against the CC-RE carried out in 10^{-3} M to 10^{-1} M KCl.

The poor repeatability between the measurements was attributed to the compression of the composite layer in the CC-RE and was the primary reason for coming up with the PC-RE design (3.4.2). Additionally, unlike the CC-ISEs that require the carbon cloth for ion-to-electron transduction, there was no need for a carbon cloth in the reference electrode. Separating the ISE(s) and reference electrode cells, as well as, using Ag/AgCl wire for the PC-RE design simplified both the manufacturing of the reference electrode and the measurement.

4.4 PVAc/KCl Composite-Based Planar Reference Electrode using PC Support (PC-RE)

4.4.1 Calibration of CC-ISEs vs. the PC-RE

The potentiometric response of three potassium and three chloride CC-ISEs were measured against the PC-RE using the flow-through setup without prior conditioning of the CC-ISEs. The results from the calibration done in 10^{-3} M to 10^{-1} M KCl solutions are displayed in Figure 27. The points shown on the graph are within-day averages and the error bars are obtained from the respective standard deviations. Appendix A and Appendix B show the individual results used to obtain the averages and standard deviations for the K-ISEs and Cl-ISEs, respectively.

The typical concentrations of K^+ and Cl^- in sweat lie within the 10^{-3} M to 10^{-1} M range[6]; hence, the good linearity and near-Nernstian response exhibited by each CC-ISE – PC-RE combination demonstrates basic suitability for their intended application. The results in Figure 27 also show a small within-day variability indicating good reliability for each calibration curve.

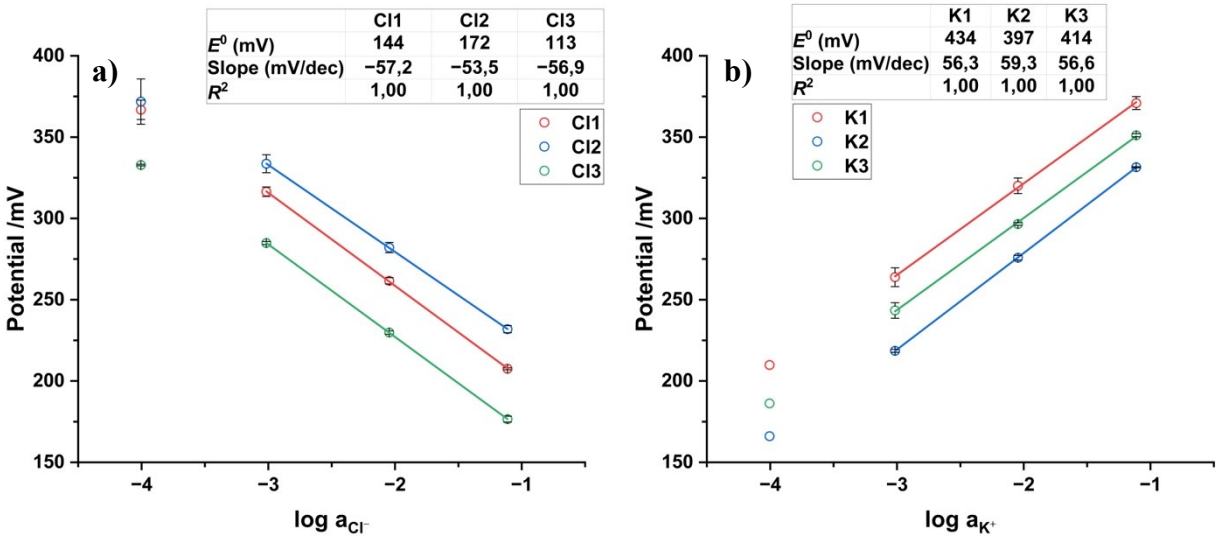

Figure 27. Calibration curves of the CC-ISEs (a: chloride; b: potassium) against the PC-RE carried out in KCl solutions using the flow-through setup.

However, the results show a major issue, poor reproducibility between electrodes. Although the electrodes were made in a similar way and were supposed to be identical, the responses, particularly the standard potentials, are highly variable. A likely cause for the poor E^0 reproducibility of the electrodes prepared in this work is the use of a method with imperfect repeatability, i.e., drop casting and manual hole punching. Automating the manufacturing

process would likely result in better E^0 reproducibility for the CC-ISEs and be a positive step towards their use as calibration-free sensors.

4.4.2 Simultaneous Calibration of K-ISE and Cl-ISE vs. the PC-RE

Between-Day Repeatability

A major advantage of the developed flow-through design is the ability to incorporate multiple ISEs for simultaneous measurement using one reference electrode. Figure 28 shows calibration plots obtained using the CC-ISEs, K1 and Cl2 electrodes, in a double-cell PC support (Figure 11) measured against the PC-RE in the flow-through setup. The plots were made using averages of the results obtained from meausrements done within three different days. The error bars show the respective standard deviations. The individual plots used to obtain the averages and standard deviations are presented in Appendix C.

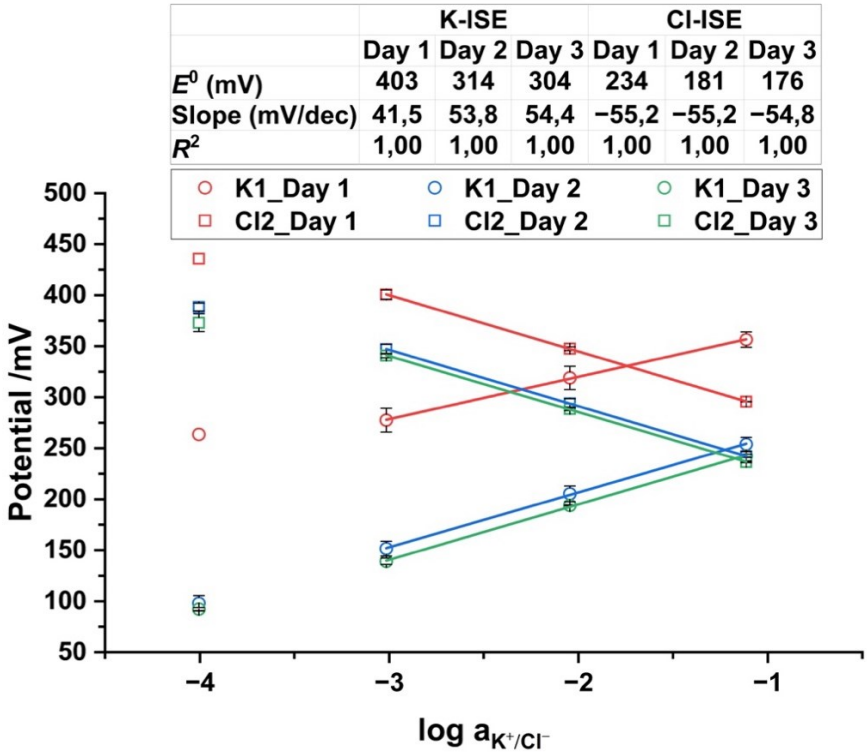

Figure 28. Calibration curves of CC-ISEs (K1 and Cl2) in a double-cell PC support measured against the PC-RE using a flow-through setup. The measurements were carried out in KCl solutions and the calibration curves were plotted using within-day averages for three different days.

The results show that the electrodes maintain a linear near-Nernstian response across different days; however, the E^0s shift significantly from day to day, a common occurance in solid-contact ISEs[73]. For most applications of macro-sized ISEs, daily calibration is necessary and acceptable; however, miniaturised ISEs are usually intended for applications where frequent

calibration is impractical such as in wearables. With the goal of calibration-free sensing in mind, this non-ideal behaviour also contributes to the expected lifetime of the electrodes during which the measured values would be reliable. Greater between-day variability would support their use as disposable sensors.

The likely cause of the between-day E^0 variability for the same electrodes is water layer formation between the ISM and CC substrate. It was shown that a water layer often forms in solid-contact ISEs at the substrate | ISM interface[74]. Although the PVC-based polymeric membrane is highly hydrophobic, some water molecules are still able to pass through to reach the substrate | ISM interface. Methods such as using a more hydrophobic ISM membrane[75] and making the solid-contact material more hydrophobic[73] have been proposed as solutions to the water layer formation but no method has been widely adopted yet. Tackling the water layer formation would increase the usability and reliability of the electrodes.

Within-Day Repeatability

The electrodes show poor E^0 reproducibility between electrodes prepared identically (Figure 27) and between the same electrodes measured on different days (Figure 28). However, Figure 27 and Figure 28 also show small error bars, indicating good within-day repeatability. The good within-day repeatability can also be seen in Figure 29, which shows the potentiometric response of K1 and Cl2 electrodes simulataneously measured three times within the same day in a double-cell against the PC-RE. The figure shows that the measured potential at each concentration is repeatable.

Another observation from Figure 29 is the instability of responses at 10^{-4} M and 10^{-5} M. In addition to the typical concentrations of K^+ and Cl^- in sweat, the observed responses in Figure 29 further support the decision to use the 10^{-3} M to 10^{-1} M range for linear calibration. Figure 29 also demonstrates the fast response of the flow-through device. For concentrations in the selected 10^{-3} M to 10^{-1} M linear range, the electrodes approach a stable response in less than 1 minute.

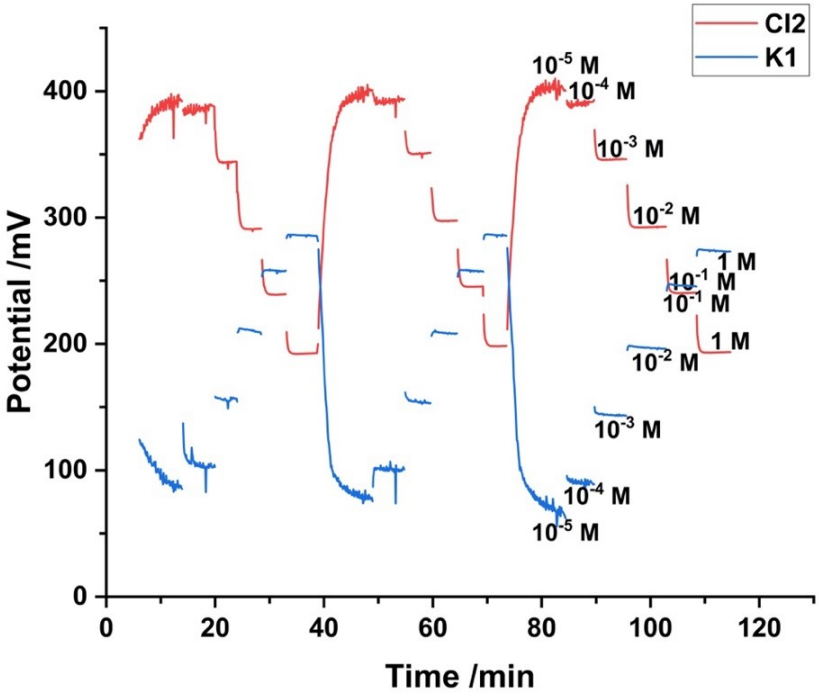

Figure 29. Within-day responses of K1 and Cl2 CC-ISEs measured against the PC-RE done from low to high concentrations of KCl solution three times.

4.4.3 Calibration in the Presence of a Background Electrolyte

The sodium ion (Na^+) is another ion present in sweat at relatively high concentrations (10 mM to 90 mM[6]). To study the effect of the presence of Na^+, the response of one potassium CC-ISE, K3, was recorded in KCl solutions with 0.1 M NaCl as background electrolyte (BGE). Results from the calibration of K3 electrode in KCl solutions with and without NaCl as BGE are presented in Figure 30. The individual plots used to obtain the averages and standard deviations are presented in Appendix D.

The curves with and without the BGE show a similar response indicating that the K-ISE response is not significantly influenced by the presence of sodium ions within the selected linear range.

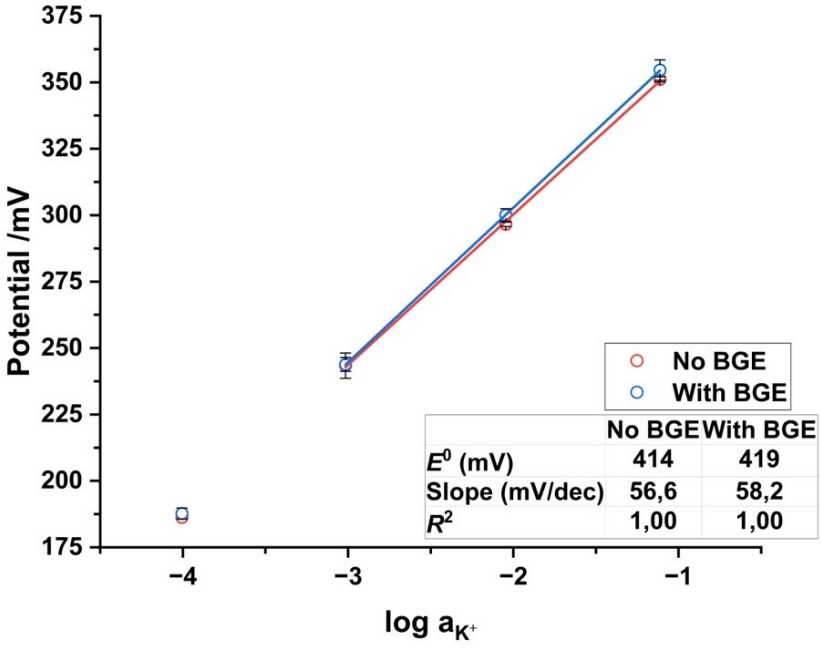

Figure 30. Calibration curves obtained for K3 electrode against the PC-RE measured in KCl solutions with and without 0.1 M NaCl as background electrolyte.

4.4.4 Selectivity Coefficient Determination

Although measuring and comparing the response of ISEs in the presence and absence of a BGE gives some information on interference by other species, calculating the selectivity coefficients is a more thorough way of evaluating interference effects. To obtain the selectivity coefficients, three replicate measurements were done using K1 and Cl2 electrodes against the PC-RE in a flow-through setup. The calculated selectivity coefficients for the electrodes in the presence of the selected interfering ions are presented in Table 3. The table also shows selectivity coefficients reported by other similar ISEs in the literature.

Table 3. Selectivity coefficients obtained using potassium and chloride ISEs prepared in this work and some previously reported selectivity coefficients from the literature. Selectivity coefficients were obtained either by SSM (*) or FIM (**).

log $K_{i,j}$	**Na^+**	**Ca^{2+}**	**Mg^{2+}**	**HCO_3^-**	**$C_3H_5O_3^-$**
[a]K-ISE (n=3)*	–3.05 ± 0.20	–4.39 ± 0.25	–4.43 ± 0.20		
[b]K-ISE[76]**	–3.9 ± 0.1	–5.5 ± 0.3	–5.6 ± 0.1		
[c]K-ISE[77]*	–3.7±0.1	–5.4 ± 0.2	–5.7 ± 0.1		
[d]K-ISE[78]**	–3.09	–3.42	–3.67		
[e]Cl-ISE (n=3)*				–0.56 ± 0.01	–0.74 ± 0.09
[f]Cl-ISE[79]*				–0.3	–0.5
[g]Cl-ISE[80]*				–1.2 ± 0.6	—

a) This study. **b)** K-ISM drop cast on carbon black-modified stencil-printed electrodes on PET substrates and measured against a poly(methyl methacrylate-co-butyl methacrylate)/KCl-based solid-state reference electrode[76]. **c)** Carbon black on glassy carbon (GC) substrate with drop cast K-ISM measured against a commercial reference electrode[77]. **d)** K-ISM drop cast on poly (3,4-ethylenedioxythiophene):polystyrene sulfonate (PEDOT:PSS) on gold substrate and measured against a PVB/NaCl reference electrode[78]. **e)** This study. **f)** Cl-ISMs prepared by the sol-gel method and measured against a commercial reference electrode[79]. **g)** PVC-based Cl-ISM drop cast on GC/PEDOT and measured against a commercial reference electrode[80].

The K-ISMs used were all based on valinomycin, and the Cl-ISMs were based on TDMAC.

The selectivity coefficients obtained in this thesis are in line with the other values from similar ISEs in the literature. Valinomycin[23] is an ionophore which has consistently shown good selectivity towards K^+; hence, the low selectivity coefficients observed are not surprising. On the other hand, TDMAC, an ion-exchanger is not regarded as highly selective towards chloride.

Developing anion-selective electrodes with high selectivity has been a major struggle. Ion-exchangers like TDMAC are used for a wide range of anions with selectivity strongly depending on the Hofmeister series[81]. The Hofmeister series basically characterizes ions according to their hydration energy or hydrophobicity[82]. Ions with a high hydrophobicity are more likely to move into the hydrophobic ISM than remain in the aqueous sample. Lactate is an organic anion, highly hydrophobic compared to Cl^- and bicarbonate has a similar level of hydrophobicity as Cl^-. With this context, the relatively poor selectivity offered by the Cl-ISE used in this thesis is reasonable.

Figure 31 shows the potential response of the CC-ISEs during one of the selectivity measurements. One important observation is that both the K- and Cl-ISEs show good

reversibility as they show a similar response to 0.1 M KCl solution before and after exposure to the interfering ions.

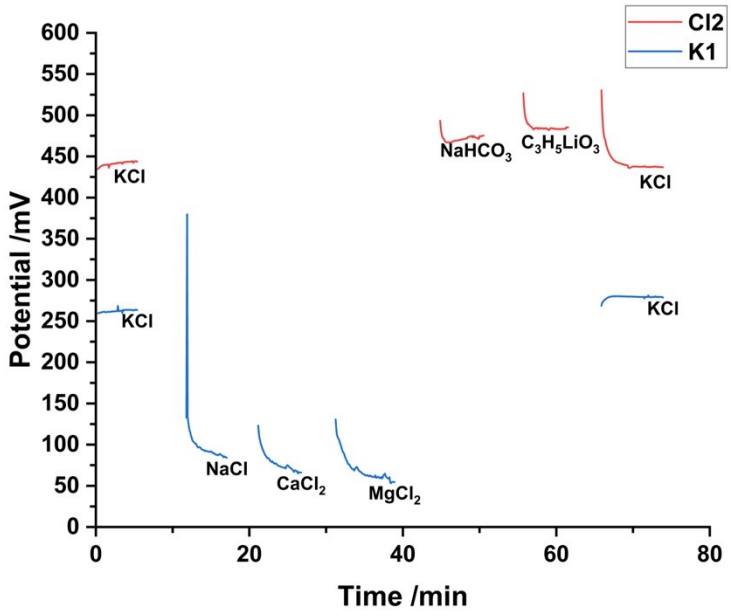

Figure 31. Potential response of K1 and Cl2 electrodes in the presence of primary and interfering ions at 0.1 M concentrations.

4.5 Electrochemical Impedance Spectroscopy Measurement

The electrochemical impedance spectroscopy measurements were done to determine and compare the resistance of the plasticized PVC-based ISMs in the fabricated potassium ISEs. As illustrated in the spectra of the CC-ISEs (K1, K2, and K3) shown in Figure 32, there are high-frequency semicircles related to the bulk resistance of the ISMs and low-frequency curves that can be attributed to the ion-to-electron transduction process. The bulk resistance of the ISMs in K1, K2, and K3 electrodes are ca. 75, 55, and 45 MΩ, respectively.

Although all three electrodes were prepared in the same way, the varying bulk resistance values indicates the weak reproducibility offered by the manual electrode fabrication. The observed resistance in previous work using the same K-ISE design but with a slightly thinner ISM[12, 13] was ca. 100 MΩ. This is higher than the values observed for the slightly thicker ISMs used in this thesis; however, it is a non-significant difference that is likely due to the previously discussed reproducibility issue with the fabrication. A thicker ISM correlates with a longer ISE lifetime; hence, the slightly thicker design used in this thesis might be more beneficial.

The resistance of valinomycin-based potassium ISMs reported in the literature is typically around 10 MΩ[83, 84] with some studies reporting values less than 1 MΩ[85, 86]. The high resistance values in this work and previous work[12, 13] could be due to the higher thickness of the ISMs in this design. However, despite the higher resistance values of the ISMs, the K-ISEs studied in this work showed fast and relatively stable responses during the potentiometric measurements (Figure 29).

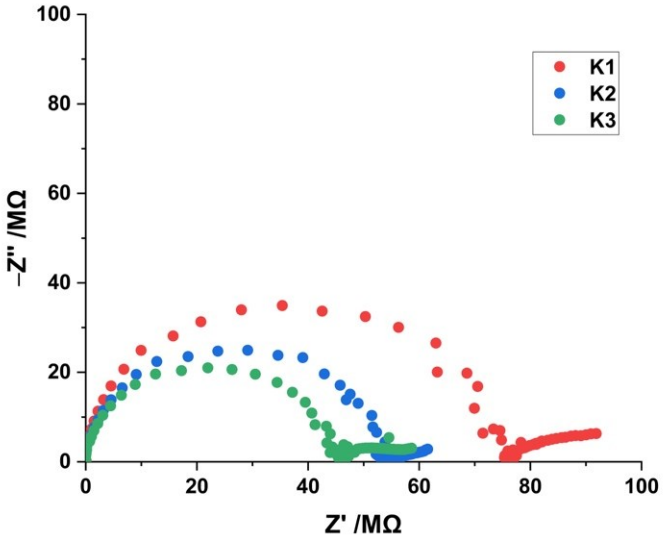

Figure 32. EIS spectra for three identical CC-ISEs (K1, K2, and K3) recorded in 0.1 M KCl solution. The spectra were recorded at open-circuit potential using 100 mV excitation amplitude in the frequency range 100 kHz to 10 mHz.

5 Conclusions

The goal of the work in this thesis was to develop a planar flow-through device for potentiometric sensing. Previous work laid the foundation by designing a carbon cloth-based potassium ion-selective electrode (K-ISE) and this work mostly built upon that by developing solid-state planar reference electrodes for a flow-through operation. The prepared flow-through cell containing combined solid-state reference and ion-selective electrodes (ISEs) continuously responded to changing ionic concentrations of aqueous solution flowing through a 2.5 mm channel. The aim of developing the flow-through device was to serve as a proof-of-concept for wearable sweat sensing. The prepared device showed fast response and good linear correlation within the concentration ranges of potassium and chloride ions in typical sweat samples.

To select a solid-state reference electrode design for the flow-through cell, the performance of two designs were tested on 3 mm silver disk electrodes. The solid-state silver/silver chloride (Ag/AgCl) reference electrodes that used a polyvinyl butyral/sodium chloride (PVB/NaCl) membrane to maintain constant chloride concentration performed worse than the Ag/AgCl reference electrode with a layer of polyvinyl acetate/potassium chloride (PVAc/KCl) composite. Hence, the PVAc/KCl composite-based reference electrode was selected for making the planar reference electrode incorporated in the flow-through cell.

In the first attempt, carbon cloth (CC) was used as a substrate together with Ag/AgCl paste that was then covered with PVAc/KCl composite. Although this design allowed the reference electrode to be included in the same cell as the ISE, the PVAc/KCl composite was easily compressed, narrowing the flow-through channel of the reference electrode. The CC-based reference electrode showed good performance when used in calibrating a commercial chloride ISE, but the compression of the composite resulted in poor performance against a K-ISE. In the second attempt, a polycarbonate (PC) cell together with Ag/AgCl wire embedded in the PVAc/KCl composite was used for making the reference electrode part. This PC-based design was easier to manufacture and solved the compression problem mentioned earlier by keeping the reference and ion-selective electrodes in separate cells.

Potassium ion-selective electrodes (K-ISEs) and chloride ion-selective electrodes (Cl-ISEs) were prepared using carbon cloth for ion-to-electron transduction. The K-ISEs were based on valinomycin, a neutral ionophore and the Cl-ISEs were based on tridodecylmethylammonium chloride (TDMAC), an ion-exchanger. When calibrated against the PC-RE, both ISE types

typically showed near-Nernstian slopes in the 10^{-3} M to 10^{-1} M KCl range with good linearity demonstrated by calibration curves with R^2 values close to 1 and good within-day repeatability demonstrated by small standard deviations. The responses of the ISEs were also fast and stable in the 10^{-3} M to 10^{-1} M KCl range. However, the electrodes displayed poor standard potential (E^0) reproducibility in between-electrode and between-day measurements.

The selectivity of the K-ISE and Cl-ISE combined with the PC-RE was also investigated using typical ions present in sweat (Na^+, Mg^+, Ca^{2+}, HCO_3^-, and $C_3H_5O_3^-$) as interfering ions. Expectedly, the K-ISE showed much better selectivity than the Cl-ISE because valinomycin strongly binds K^+ selectively while TDMAC is capable of ion-exchange with a wide range of anions. The K-ISE was also calibrated in the presence of 0.1 M NaCl background electrolyte (BGE). The calibration curve was very similar to that obtained in the absence of the BGE, further indicating the excellent selectivity of the K-ISE in the presence of Na^+, an ion present at high concentrations in sweat.

As a proof-of-concept, the device developed here showed some promising results to build on. The typical concentrations of K^+ and Cl^- in sweat lie within the linear range of the device. The PC-RE design allows for easy combination with multiple ISEs in a separate cell thereby extending the range of potential ions that can be analysed. The PVAc/KCl composite-based PC-RE also exhibited a long lifetime which can be attributed to the high chloride concentration in the PVAc/KCl composite and low salt leakage from the composite.

The major problems with the device resulted from irreproducibility in fabricating the electrodes, coming primarily from the manual fabrication. The poor fabrication reproducibility of the electrodes was evidenced by the differences in the E^0 values and ion-selective membrane (ISM) bulk resistance values of electrodes made in a similar way. The next observed issue is poor between-day reproducibility, a common issue among solid-contact ISEs, usually attributed to the formation of a water layer between the ISM and the underneath substrate.

The device has the potential for further miniaturisation and multiple ion sensing. Automated manufacturing could help to reduce the between-electrode variability. With the good within-day repeatability, the device could be used as a disposable sensor thereby bypassing the issues associated with long-term E^0 drift. To establish reliability of the sensor's lifetime, and other performance parameters, more extensive validation using simulated and real sweat samples would be required.

6 References

[1] Laricchia, F. Wearables - statistics & facts https://www.statista.com/topics/1556/wearable-technology/#topicOverview (accessed Apr 7, 2023).

[2] Kogure, M.; Nakaya, N.; Hirata, T.; Tsuchiya, N.; Nakamura, T.; Narita, A.; Suto, Y.; Honma, Y.; Sasaki, H.; Miyagawa, K.; et al. Sodium/Potassium Ratio Change Was Associated with Blood Pressure Change: Possibility of Population Approach for Sodium/Potassium Ratio Reduction in Health Checkup. *Hypertension Research*, **2021**, *44* (2), 225–231. https://doi.org/10.1038/s41440-020-00536-7.

[3] Scurati-Manzoni, E.; Fossali, E. F.; Agostoni, C.; Riva, E.; Simonetti, G. D.; Zanolari-Calderari, M.; Bianchetti, M. G.; Lava, S. A. G. Electrolyte Abnormalities in Cystic Fibrosis: Systematic Review of the Literature. *Pediatric Nephrology*, **2014**, *29* (6), 1015–1023. https://doi.org/10.1007/s00467-013-2712-4.

[4] Tang, Y.-M.; Wang, D.-G.; Li, J.; Li, X.-H.; Wang, Q.; Liu, N.; Liu, W.-T.; Li, Y.-X. Relationships between Micronutrient Losses in Sweat and Blood Pressure among Heat-Exposed Steelworkers. *Ind Health*, **2016**, *54* (3), 215–223. https://doi.org/10.2486/indhealth.2014-0225.

[5] LeGrys, V. A.; Yankaskas, J. R.; Quittell, L. M.; Marshall, B. C.; Mogayzel, P. J. Diagnostic Sweat Testing: The Cystic Fibrosis Foundation Guidelines. *J Pediatr*, **2007**, *151* (1), 85–89. https://doi.org/10.1016/j.jpeds.2007.03.002.

[6] Baker, L. B. Physiology of Sweat Gland Function: The Roles of Sweating and Sweat Composition in Human Health. *Temperature*, **2019**, *6* (3), 211–259. https://doi.org/10.1080/23328940.2019.1632145.

[7] Lee, J.; Kim, M. C.; Soltis, I.; Lee, S. H.; Yeo, W. Advances in Electrochemical Sensors for Detecting Analytes in Biofluids. *Advanced Sensor Research*, **2023**, 2200088. https://doi.org/10.1002/adsr.202200088.

[8] Moya, A.; Pol, R.; Martínez-Cuadrado, A.; Villa, R.; Gabriel, G.; Baeza, M. Stable Full-Inkjet-Printed Solid-State Ag/AgCl Reference Electrode. *Anal Chem*, **2019**, *91* (24), 15539–15546. https://doi.org/10.1021/acs.analchem.9b03441.

[9] Hoekstra, R.; Blondeau, P.; Andrade, F. J. IonSens: A Wearable Potentiometric Sensor Patch for Monitoring Total Ion Content in Sweat. *Electroanalysis*, **2018**, *30* (7), 1536–1544. https://doi.org/10.1002/elan.201800128.

[10] Liu, C.; Xu, T.; Wang, D.; Zhang, X. The Role of Sampling in Wearable Sweat Sensors. *Talanta*, **2020**, *212*, 120801. https://doi.org/https://doi.org/10.1016/j.talanta.2020.120801.

[11] Gao, F.; Liu, C.; Zhang, L.; Liu, T.; Wang, Z.; Song, Z.; Cai, H.; Fang, Z.; Chen, J.; Wang, J.; et al. Wearable and Flexible Electrochemical Sensors for Sweat Analysis: A Review. *Microsyst Nanoeng*, **2023**, *9* (1), 1. https://doi.org/10.1038/s41378-022-00443-6.

[12] Guagneli, L. Novel Design of a Flow-through Potentiometric Sensing Device, Åbo Akademi, 2021.

[13] Guagneli, L.; Mousavi, Z.; Sokalski, T.; Leito, I.; Bobacka, J. Novel Design of a Planar Flow-through Potentiometric Sensor. *Journal of Electroanalytical Chemistry*, **2022**, *923*, 116785. https://doi.org/10.1016/j.jelechem.2022.116785.

[14] Mousavi, Z.; Granholm, K.; Sokalski, T.; Lewenstam, A. An Analytical Quality Solid-State Composite Reference Electrode. *Analyst*, **2013**, *138* (18), 5216–5220. https://doi.org/10.1039/C3AN00852E.

[15] Granholm, K.; Mousavi, Z.; Sokalski, T.; Lewenstam, A. Analytical Quality Solid-State Composite Reference Electrode Manufactured by Injection Moulding. *Journal of Solid State Electrochemistry*, **2014**, *18* (3), 607–612. https://doi.org/10.1007/s10008-013-2294-x.

[16] Hulanicki, A.; Glab, S.; Ingman, F. Chemical Sensors: Definitions and Classification. *Pure and applied chemistry*, **1991**, *63* (9), 1247–1250.

[17] Janata, J. *Principles of Chemical Sensors*; Springer US: Boston, MA, 2009. https://doi.org/10.1007/b136378.

[18] Eggins, B. R. *Chemical Sensors and Biosensors*; Ando, D. J., Ed.; Analytical Techniques in the Sciences (AnTs); John Wiley & Sons, LTD, 2002.

[19] Hu, J.; Stein, A.; Bühlmann, P. Rational Design of All-Solid-State Ion-Selective Electrodes and Reference Electrodes. *TrAC Trends in Analytical Chemistry*, **2016**, *76*, 102–114. https://doi.org/10.1016/j.trac.2015.11.004.

[20] Mikhelson, K. N. Introductory Issues. In *Ion-Selective Electrodes*; Mikhelson, K. N., Ed.; Springer Berlin Heidelberg: Berlin, Heidelberg, 2013; pp 1–10. https://doi.org/10.1007/978-3-642-36886-8_1.

[21] Buck, R. P.; Lindner, E. Recommendations for Nomenclature of Ionselective Electrodes (IUPAC Recommendations 1994). **1994**, *66* (12), 2527–2536. https://doi.org/10.1351/pac199466122527.

[22] Wang, J. Potentiometry. In *Analytical Electrochemistry*; John Wiley & Sons, Inc.: Hoboken, NJ, USA, 2006; pp 165–200. https://doi.org/10.1002/0471790303.ch5.

[23] Pioda, L. A. R.; Stankova, V.; Simon, W. Highly Selective Potassium Ion Responsive Liquid-Membrane Electrode. *Anal Lett*, **1969**, *2* (12), 665–674. https://doi.org/10.1080/00032716908051343.

[24] Ammann, D.; Pretsch, E.; Simon, W.; Lindner, E.; Bezegh, A.; Pungor, E. Lipophilic Salts as Membrane Additives and Their Influence on the Properties of Macro- and Micro-Electrodes Based on Neutral Carriers. *Anal Chim Acta*, **1985**, *171* (C), 119–129. https://doi.org/10.1016/S0003-2670(00)84189-6.

[25] Zareh, M. M. Plasticizers and Their Role in Membrane Selective Electrodes. In *Recent Advances in Plasticizers*; 2012; pp 113–124.

[26] National Center for Biotechnology Information. PubChem Compound Summary for CID 6338, Vinyl Chloride https://pubchem.ncbi.nlm.nih.gov/compound/Vinyl-Chloride (accessed Apr 25, 2023).

[27] National Center for Biotechnology Information. PubChem Compound Summary for CID 5649, Valinomycin https://pubchem.ncbi.nlm.nih.gov/compound/Valinomycin (accessed Apr 5, 2023).

[28] National Center for Biotechnology Information. PubChem Compound Summary for CID 23694899, Potassium tetrakis[3,5-bis(trifluoromethyl)phenyl]borate https://pubchem.ncbi.nlm.nih.gov/compound/23694899 (accessed Apr 25, 2023).

[29] National Center for Biotechnology Information. PubChem Compound Summary for CID 31218, Bis(2-ethylhexyl) sebacate https://pubchem.ncbi.nlm.nih.gov/compound/Bis_2-ethylhexyl_-sebacate (accessed Apr 25, 2023).

[30] National Center for Biotechnology Information. PubChem Compound Summary for CID 169952, 2-Nitrophenyl octyl ether https://pubchem.ncbi.nlm.nih.gov/compound/2-Nitrophenyl-octyl-ether (accessed Apr 25, 2023).

[31] National Center for Biotechnology Information. PubChem Compound Summary for CID 81601, Tridodecylmethylammonium chloride https://pubchem.ncbi.nlm.nih.gov/compound/Tridodecylmethylammonium-chloride (accessed Apr 25, 2023).

[32] National Center for Biotechnology Information. PubChem Compound Summary for CID 8028, Tetrahydrofuran https://pubchem.ncbi.nlm.nih.gov/compound/Tetrahydrofuran (accessed Apr 25, 2023).

[33] Hu, J.; Stein, A.; Bühlmann, P. Rational Design of All-Solid-State Ion-Selective Electrodes and Reference Electrodes. *TrAC Trends in Analytical Chemistry*, **2016**, *76*, 102–114. https://doi.org/10.1016/j.trac.2015.11.004.

[34] Lyu, Y.; Gan, S.; Bao, Y.; Zhong, L.; Xu, J.; Wang, W.; Liu, Z.; Ma, Y.; Yang, G.; Niu, L. Solid-Contact Ion-Selective Electrodes: Response Mechanisms, Transducer Materials and Wearable Sensors. *Membranes (Basel)*, **2020**, *10* (6). https://doi.org/10.3390/membranes10060128.

[35] Cattrall, R. W.; Freiser, Henry. Coated Wire Ion-Selective Electrodes. *Anal Chem*, **1971**, *43* (13), 1905–1906. https://doi.org/10.1021/ac60307a032.

[36] James, H. J.; Carmack, Gary.; Freiser, Henry. Coated Wire Ion-Selective Electrodes. *Anal Chem*, **1972**, *44* (4), 856–857. https://doi.org/10.1021/ac60312a046.

[37] Lai, C.-Z.; Fierke, M. A.; Stein, A.; Bühlmann, P. Ion-Selective Electrodes with Three-Dimensionally Ordered Macroporous Carbon as the Solid Contact. *Anal Chem*, **2007**, *79* (12), 4621–4626. https://doi.org/10.1021/ac070132b.

[38] Crespo, G. A.; Macho, S.; Rius, F. X. Ion-Selective Electrodes Using Carbon Nanotubes as Ion-to-Electron Transducers. *Anal Chem*, **2008**, *80* (4), 1316–1322. https://doi.org/10.1021/ac071156l.

[39] Li, F.; Ye, J.; Zhou, M.; Gan, S.; Zhang, Q.; Han, D.; Niu, L. All-Solid-State Potassium-Selective Electrode Using Graphene as the Solid Contact. *Analyst*, **2012**, *137* (3), 618–623. https://doi.org/10.1039/C1AN15705A.

[40] Fouskaki, M.; Chaniotakis, N. Fullerene-Based Electrochemical Buffer Layer for Ion-Selective Electrodes. *Analyst*, **2008**, *133* (8), 1072–1075. https://doi.org/10.1039/B719759D.

[41] Mattinen, U.; Rabiej, S.; Lewenstam, A.; Bobacka, J. Impedance Study of the Ion-to-Electron Transduction Process for Carbon Cloth as Solid-Contact Material in Potentiometric Ion Sensors. *Electrochim Acta*, **2011**, *56* (28), 10683–10687. https://doi.org/10.1016/j.electacta.2011.07.082.

[42] Bobacka, J. Conducting Polymer-Based Solid-State Ion-Selective Electrodes. *Electroanalysis*, **2006**, *18* (1), 7–18. https://doi.org/10.1002/elan.200503384.

[43] Cadogan, Aodhmar.; Gao, Zhiqiang.; Lewenstam, Andrzej.; Ivaska, Ari.; Diamond, Dermot. All-Solid-State Sodium-Selective Electrode Based on a Calixarene Ionophore in a Poly(Vinyl Chloride) Membrane with a Polypyrrole Solid Contact. *Anal Chem*, **1992**, *64* (21), 2496–2501. https://doi.org/10.1021/ac00045a007.

[44] *Handbook of Reference Electrodes*; Inzelt, G., Lewenstam, A., Scholz, F., Eds.; Springer Berlin Heidelberg: Berlin, Heidelberg, 2013. https://doi.org/10.1007/978-3-642-36188-3.

[45] Harris, D. C. *Quantitative Chemical Analysis*, Seventh Edition.; W.H. Freeman and Co.: New York, 2007.

[46] Shinwari, M. W.; Zhitomirsky, D.; Deen, I. A.; Selvaganapathy, P. R.; Deen, M. J.; Landheer, D. Microfabricated Reference Electrodes and Their Biosensing Applications. *Sensors*, **2010**, *10* (3), 1679–1715. https://doi.org/10.3390/s100301679.

[47] Diamond, D.; McEnroe, E.; McCarrick, M.; Lewenstam, A. Evaluation of a New Solid-State Reference Electrode Junction Material for Ion-Selective Electrodes. *Electroanalysis*, **1994**, *6* (11–12), 962–971. https://doi.org/10.1002/elan.1140061108.

[48] Mattinen, U.; Bobacka, J.; Lewenstam, A. Solid-Contact Reference Electrodes Based on Lipophilic Salts. *Electroanalysis*, **2009**, *21* (17–18), 1955–1960. https://doi.org/10.1002/elan.200904615.

[49] Mamińska, R.; Dybko, A.; Wróblewski, W. All-Solid-State Miniaturised Planar Reference Electrodes Based on Ionic Liquids. *Sens Actuators B Chem*, **2006**, *115* (1), 552–557. https://doi.org/10.1016/j.snb.2005.10.018.

[50] National Center for Biotechnology Information. PubChem Compound Summary for CID 5234, Sodium Chloride https://pubchem.ncbi.nlm.nih.gov/compound/Sodium-Chloride (accessed Apr 9, 2023).

[51] Gao, W.; Emaminejad, S.; Nyein, H. Y. Y.; Challa, S.; Chen, K.; Peck, A.; Fahad, H. M.; Ota, H.; Shiraki, H.; Kiriya, D.; et al. Fully Integrated Wearable Sensor Arrays for Multiplexed in Situ Perspiration Analysis. *Nature*, **2016**, *529* (7587), 509–514. https://doi.org/10.1038/nature16521.

[52] Zamarayeva, A. M.; Yamamoto, N. A. D.; Toor, A.; Payne, M. E.; Woods, C.; Pister, V. I.; Khan, Y.; Evans, J. W.; Arias, A. C. Optimization of Printed Sensors to Monitor Sodium, Ammonium, and Lactate in Sweat. *APL Mater*, **2020**, *8* (10), 100905. https://doi.org/10.1063/5.0014836.

[53] McMahon, G. *Analytical Instrumentation: A Guide to Laboratory, Portable and Miniaturized Instruments*; Wiley-Interscience, 2007.

[54] Willard, H. H.; Merritt, L. L. J.; Dean, J. A.; Settle, F. A. J. *Instrumental Methods of Analysis*, Seventh edition.; Wadsworth Publishing Company: Belmont, California, 1988.

[55] Makarychev-Mikhailov, S.; Shvarev, A.; Bakker, E. New Trends in Ion-Selective Electrodes. In *Electrochemical Sensors, Biosensors and their Biomedical Applications*; Elsevier, 2008; pp 71–114. https://doi.org/10.1016/B978-012373738-0.50006-4.

[56] *The IUPAC Compendium of Chemical Terminology*; International Union of Pure and Applied Chemistry (IUPAC): Research Triangle Park, NC, 2019. https://doi.org/10.1351/goldbook.

[57] Gadzekpo, V. P. Y.; Christian, G. D. Determination of Selectivity Coefficients of Ion-Selective Electrodes by a Matched-Potential Method. *Anal Chim Acta*, **1984**, *164*, 279–282. https://doi.org/10.1016/S0003-2670(00)85640-8.

[58] Sokalski, T.; Maj-Żurawska, M.; Hulanicki, A. Determination of True Selectivity Coefficients of Neutral Carrier Calcium Selective Electrode. *Mikrochim Acta*, **1991**, *103* (5–6), 285–291. https://doi.org/10.1007/BF01243265.

[59] Miyake, M.; Chen, L. D.; Pozzi, G.; Bühlmann, P. Ion-Selective Electrodes with Unusual Response Functions: Simultaneous Formation of Ionophore–Primary Ion Complexes with Different Stoichiometries. *Anal Chem*, **2012**, *84* (2), 1104–1111. https://doi.org/10.1021/ac202761x.

[60] Han, T.; Kalinichev, A. V.; Mousavi, Z.; Mikhelson, K. N.; Bobacka, J. Anomalous Potentiometric Response of Solid-Contact Ion-Selective Electrodes with Thin-Layer Membranes. *Sens Actuators B Chem*, **2022**, *357*, 131416. https://doi.org/10.1016/j.snb.2022.131416.

[61] De Marco, R.; Clarke, G.; Pejcic, B. Ion-Selective Electrode Potentiometry in Environmental Analysis. *Electroanalysis*, **2007**, *19* (19–20), 1987–2001. https://doi.org/10.1002/elan.200703916.

[62] Light, T. S. Industrial Use and Applications of Ion Selective Electrodes. *J Chem Educ*, **1997**, *74* (2), 171. https://doi.org/10.1021/ed074p171.

[63] Lewenstam, A.; Maj-Zurawska, M.; Hulanicki, A. Application of Ion-Selective Electrodes in Clinical Analysis. *Electroanalysis*, **1991**, *3* (8), 727–734. https://doi.org/10.1002/elan.1140030802.

[64] Mikhelson, K. N. ISE Constructions; 2013; pp 135–148. https://doi.org/10.1007/978-3-642-36886-8_8.

[65] Thermo Scientific Konelab 20 https://pdf.medicalexpo.com/pdf/thermo-scientific/konelab-20/78678-85059.html (accessed May 17, 2023).

[66] Zachara, J.; Wróblewski, W. Design and Performance of Some Microflow-Cell Potentiometric Transducers. *Analyst*, **2003**, *128* (6), 532–536. https://doi.org/10.1039/B300069A.

[67] Yang, D. S.; Ghaffari, R.; Rogers, J. A. Sweat as a Diagnostic Biofluid. *Science (1979)*, **2023**, *379* (6634), 760–761. https://doi.org/10.1126/science.abq5916.

[68] Gamry Instruments. Basics of Electrochemical Impedance Spectroscopy https://www.gamry.com/application-notes/EIS/basics-of-electrochemical-impedance-spectroscopy/ (accessed May 12, 2023).

[69] Magar, H. S.; Hassan, R. Y. A.; Mulchandani, A. Electrochemical Impedance Spectroscopy (EIS): Principles, Construction, and Biosensing Applications. *Sensors*, **2021**, *21* (19), 6578. https://doi.org/10.3390/s21196578.

[70] Anderson, E. L.; Bühlmann, P. Electrochemical Impedance Spectroscopy of Ion-Selective Membranes: Artifacts in Two-, Three-, and Four-Electrode Measurements. *Anal Chem*, **2016**, *88* (19), 9738–9745. https://doi.org/10.1021/acs.analchem.6b02641.

[71] Demoz, A.; Verpoorte, E. M. J.; Harrison, D. J. An Equivalent Circuit Model of Ion-Selective Membrane|insulator|semiconductor Interfaces Used for Chemical Sensors. *Journal of Electroanalytical Chemistry*, **1995**, *389* (1–2), 71–78. https://doi.org/10.1016/0022-0728(95)03836-6.

[72] Kielland, J. Individual Activity Coefficients of Ions in Aqueous Solutions. *J Am Chem Soc*, **1937**, *59* (9), 1675–1678. https://doi.org/10.1021/ja01288a032.

[73] Papp, S.; Bojtár, M.; Gyurcsányi, R. E.; Lindfors, T. Potential Reproducibility of Potassium-Selective Electrodes Having Perfluorinated Alkanoate Side Chain Functionalized Poly(3,4-Ethylenedioxytiophene) as a Hydrophobic Solid Contact. *Anal Chem*, **2019**, *91* (14), 9111–9118. https://doi.org/10.1021/acs.analchem.9b01587.

[74] Fibbioli, M.; Morf, W. E.; Badertscher, M.; de Rooij, N. F.; Pretsch, E. Potential Drifts of Solid-Contacted Ion-Selective Electrodes Due to Zero-Current Ion Fluxes Through the Sensor Membrane. *Electroanalysis*, **2000**, *12* (16), 1286–1292. https://doi.org/10.1002/1521-4109(200011)12:16<1286::AID-ELAN1286>3.0.CO;2-Q.

[75] Veder, J.-P.; De Marco, R.; Clarke, G.; Chester, R.; Nelson, A.; Prince, K.; Pretsch, E.; Bakker, E. Elimination of Undesirable Water Layers in Solid-Contact Polymeric Ion-Selective Electrodes. *Anal Chem*, **2008**, *80* (17), 6731–6740. https://doi.org/10.1021/ac800823f.

[76] Ozer, T.; Agir, I.; Henry, C. S. Low-Cost Internet of Things (IoT)-Enabled a Wireless Wearable Device for Detecting Potassium Ions at the Point of Care. *Sens Actuators B Chem*, **2022**, *365*, 131961. https://doi.org/10.1016/j.snb.2022.131961.

[77] Paczosa-Bator, B. All-Solid-State Selective Electrodes Using Carbon Black. *Talanta*, **2012**, *93*, 424–427. https://doi.org/10.1016/j.talanta.2012.02.013.

[78] Liu, H.; Gu, Z.; Zhao, Q.; Li, S.; Ding, X.; Xiao, X.; Xiu, G. Printed Circuit Board Integrated Wearable Ion-Selective Electrode with Potential Treatment for Highly Repeatable Sweat Monitoring. *Sens Actuators B Chem*, **2022**, *355*, 131102. https://doi.org/10.1016/j.snb.2021.131102.

[79] Kim, W.; Park, S. B.; Kim, W.; Sung, D. D.; Cha, G. S. Chloride-Selective Membranes Prepared with Different Matrices Including Polymers Obtained by the Sol–Gel Method. *Analyst*, **1998**, *123* (2), 379–382. https://doi.org/10.1039/a705788a.

[80] Sjöberg-Eerola, P.; Bobacka, J.; Lewenstam, A.; Ivaska, A. All-Solid-State Chloride Sensors Based on Electronically Conducting, Semiconducting and Insulating Polymer Membranes. *Sens Actuators B Chem*, **2007**, *127* (2), 545–553. https://doi.org/10.1016/j.snb.2007.05.004.

[81] Wegmann, D.; Weiss, H.; Ammann, D.; Morf, W. E.; Pretsch, E.; Sugahara, K.; Simon, W. Anion-Selective Liquid Membrane Electrodes Based on Lipophilic Quaternary Ammonium Compounds. *Mikrochim Acta*, **1984**, *84* (1–2), 1–16. https://doi.org/10.1007/BF01204153.

[82] Mikhelson, K. N. Ionophore-Based ISEs; 2013; pp 51–95. https://doi.org/10.1007/978-3-642-36886-8_4.

[83] Mousavi, Z.; Bobacka, J.; Lewenstam, A.; Ivaska, A. Poly(3,4-Ethylenedioxythiophene) (PEDOT) Doped with Carbon Nanotubes as Ion-to-Electron Transducer in Polymer Membrane-Based Potassium Ion-Selective Electrodes. *Journal of Electroanalytical Chemistry*, **2009**, *633* (1), 246–252. https://doi.org/10.1016/j.jelechem.2009.06.005.

[84] Ping, J.; Wang, Y.; Wu, J.; Ying, Y. Development of an All-Solid-State Potassium Ion-Selective Electrode Using Graphene as the Solid-Contact Transducer. *Electrochem commun*, **2011**, *13* (12), 1529–1532. https://doi.org/10.1016/j.elecom.2011.10.018.

[85] Mousavi, Z.; Teter, A.; Lewenstam, A.; Maj-Zurawska, M.; Ivaska, A.; Bobacka, J. Comparison of Multi-Walled Carbon Nanotubes and Poly(3-Octylthiophene) as Ion-to-Electron Transducers in All-Solid-State Potassium Ion-Selective Electrodes. *Electroanalysis*, **2011**, *23* (6), 1352–1358. https://doi.org/10.1002/elan.201000747.

[86] Tran, T. N. T.; Qiu, S.; Chung, H.-J. Potassium Ion Selective Electrode Using Polyaniline and Matrix-Supported Ion-Selective PVC Membrane. *IEEE Sens J*, **2018**, *18* (22), 9081–9087. https://doi.org/10.1109/JSEN.2018.2871001.

7 Appendices

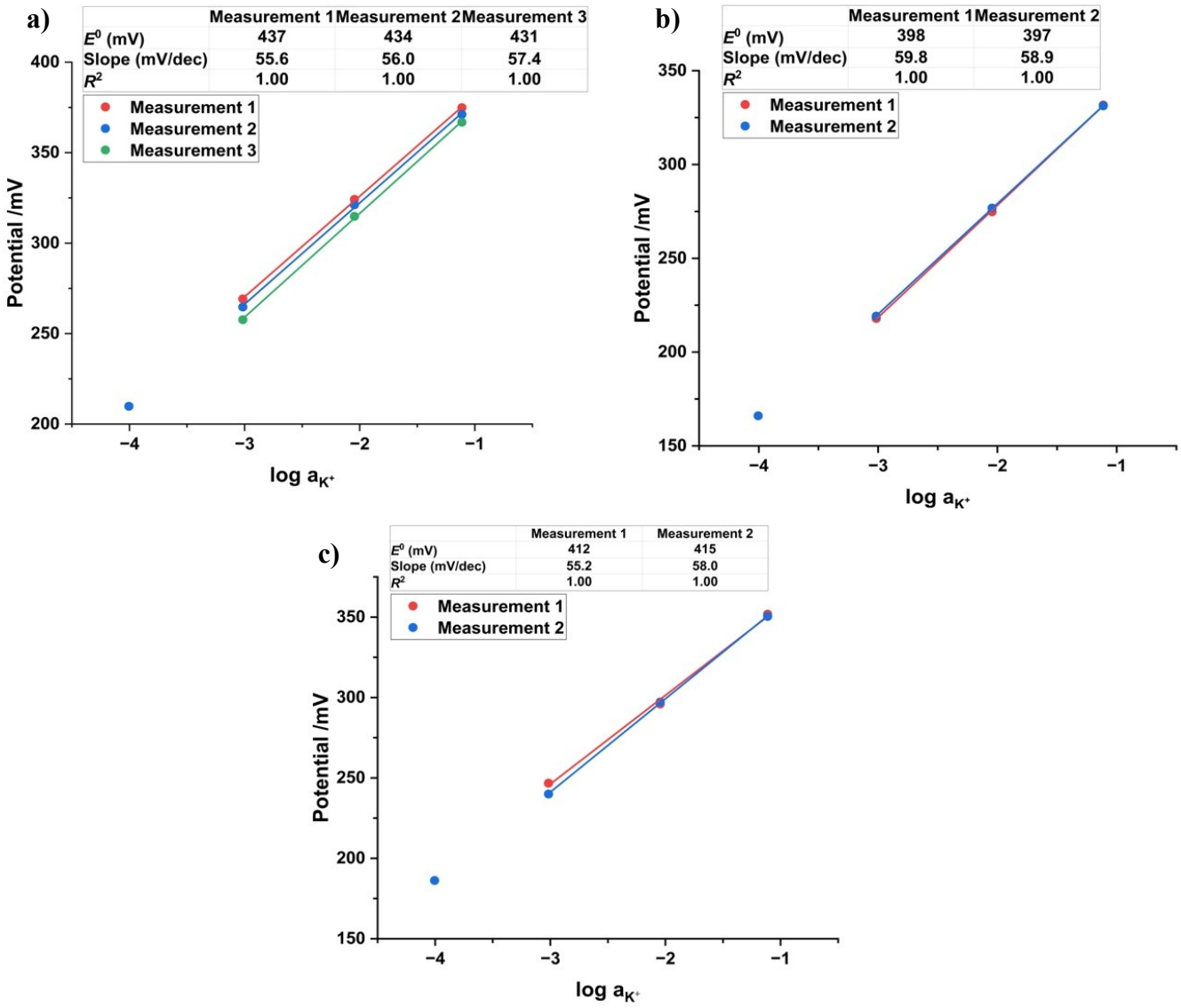

Appendix A. Individual calibration curves for K-ISEs against the PC-RE: a) K1; b) K2 c) K3.

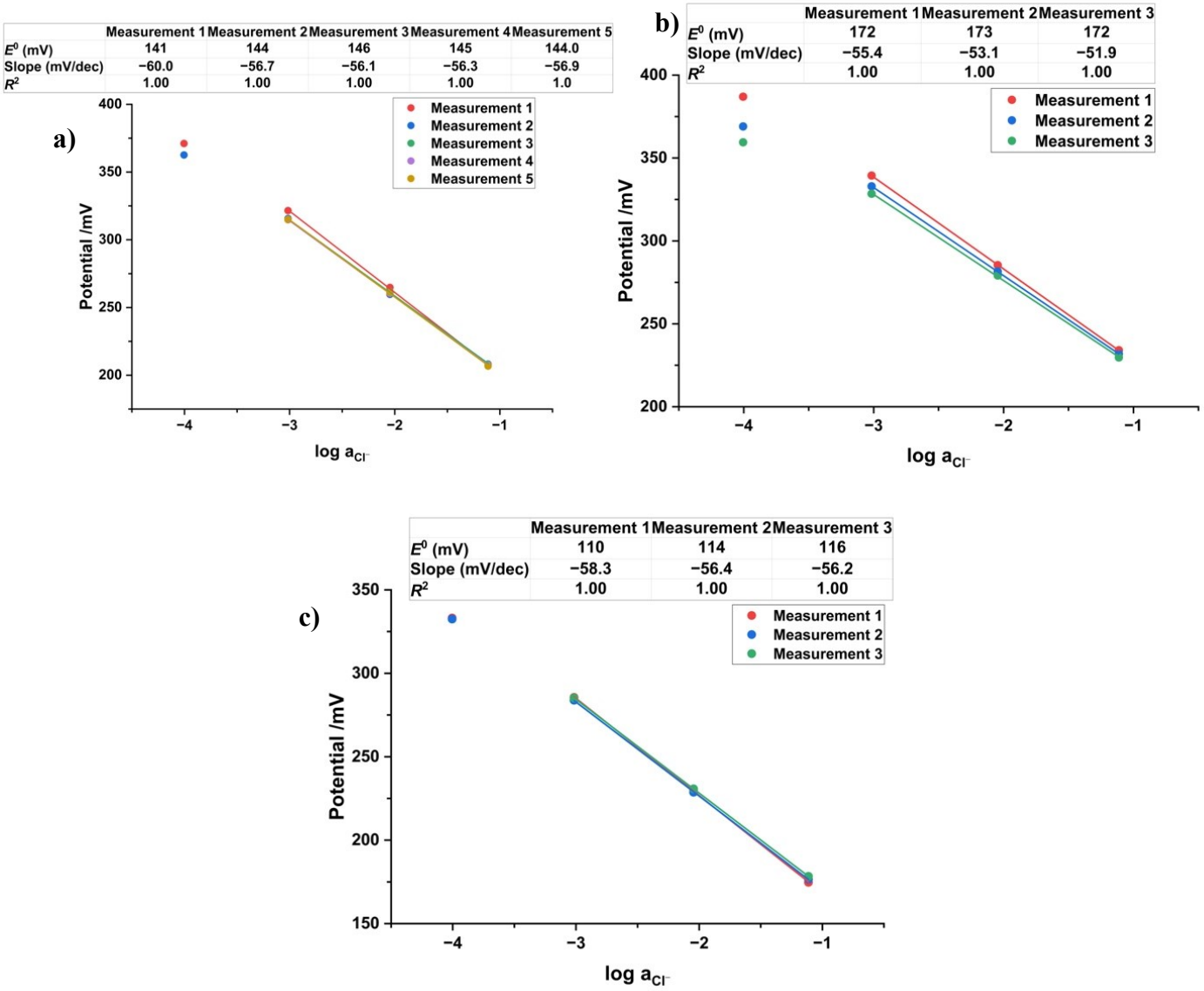

Appendix B. Individual calibration curves for Cl-ISEs against the PC-RE: a) Cl1; b) Cl2 c) Cl3.

a)

	K-ISE		CI-ISE	
	Measurement 1	Measurement 2	Measurement 1	Measurement 2
E^0 (mV)	407	399	236	233
Slope (mV/dec)	39.9	43.0	−53.6	−56.8
R^2	1.00	1.00	1.00	1.00

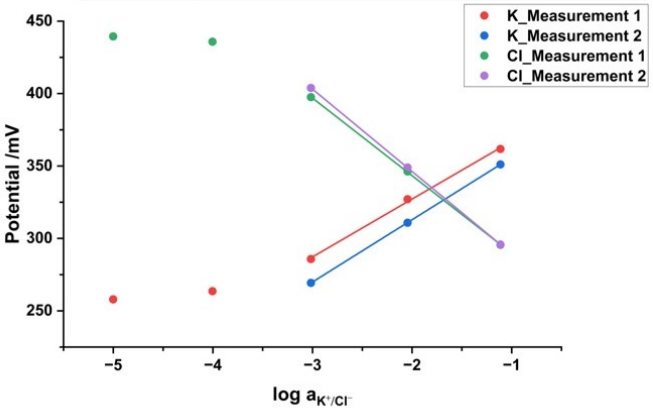

b)

	K-ISE			CI-ISE		
	Measurement 1	Measurement 2	Measurement 3	Measurement 1	Measurement 2	Measurement 3
E^0 (mV)	318	319	306	178	184	178
Slope (mV/dec)	53.0	54.4	53.9	−55.1	−55.3	−55.6
R^2	1.00	1.00	1.00	1.00	1.00	1.00

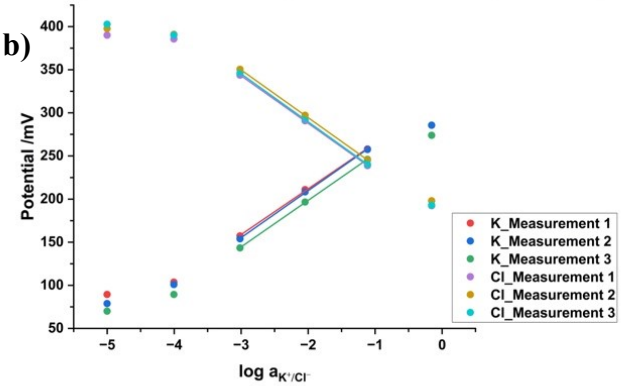

c)

	K-ISE		CI-ISE	
	Measurement 1	Measurement 2	Measurement 1	Measurement 2
E^0 (mV)	307	300	176	176
Slope (mV/dec)	56.2	52.6	−54.3	−55.4
R^2	1.00	1.00	1.00	1.00

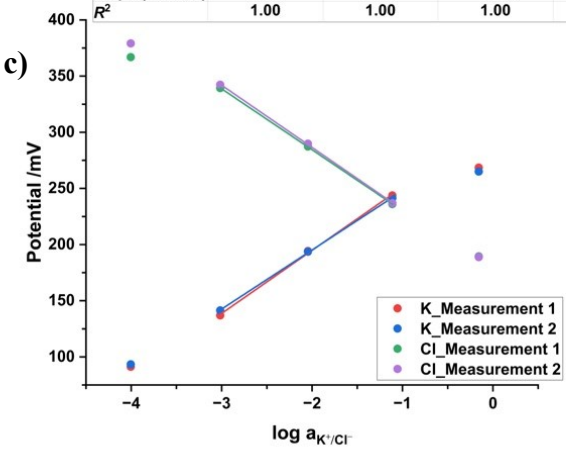

Appendix C. Individual calibration curves for K1 and Cl2 combined in a double cell and measured against the PC-RE. a) Day 1; b) Day 2; c) Day 3.

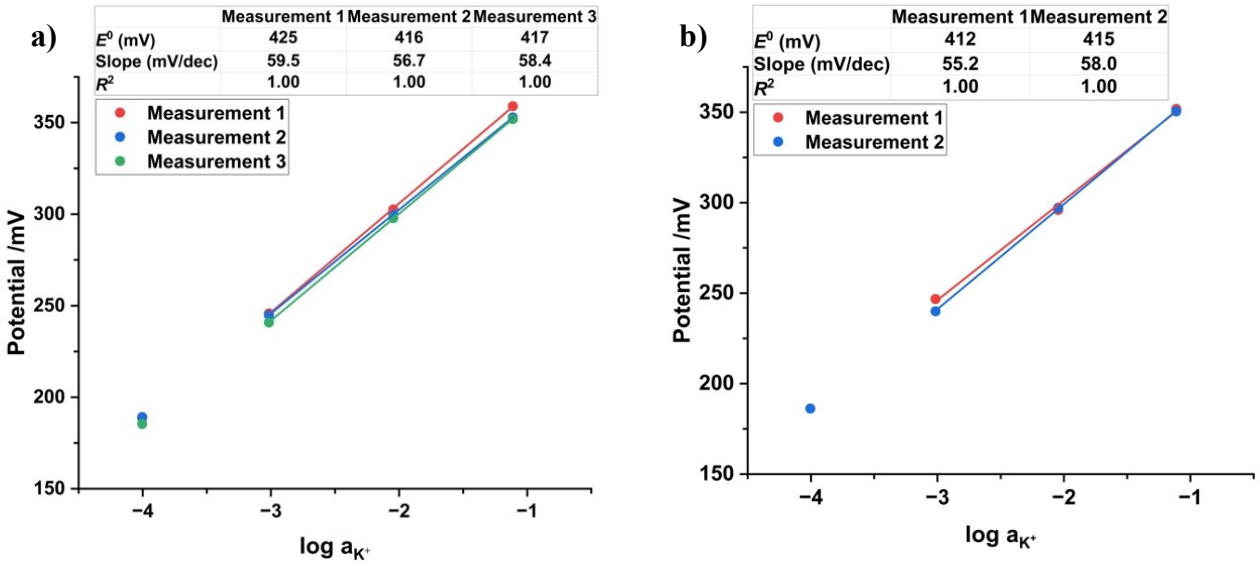

Appendix D. Individual calibration curves for measurement of K3 against the PC-RE. a) With BGE; b) No BGE. The BGE was 0.1 M NaCl.